On Translucent Yttria Stabilized Zirconia Ceramics:

Mechanical Considerations, Phase Transformation, and Cement Choices

Sebastian Franco-Tabares

Department of Prosthodontics/Dental Materials Science
Institute of Odontology
Sahlgrenska Academy, University of Gothenburg

Sweden

UNIVERSITY OF GOTHENBURG

Cover illustration:
"Crown of The Sun" by Sebastian Franco-Tabares.

Illustrations in the thesis made by Sebastian Franco-Tabares

On Translucent Yttria Stabilized Zirconia Ceramics:
Mechanical Considerations, Phase Transformation, and Cement Choices

sebastian.franco.tabares@gu.se

ISBN 978-91-7833-862-7 (PRINT)
ISBN 978-91-7833-863-4 (PDF)

Printed in Borås, Sweden 2020
Printed by Stema Specialtryck AB

On Translucent Yttria Stabilized Zirconia Ceramics:

Mechanical Considerations, Phase Transformation, and Cement Choices

Sebastian Franco-Tabares
Department of Prosthodontics/Dental Materials Science, Institute of Odontology. Sahlgrenska Academy, University of Gothenburg
Gothenburg, Sweden

ABSTRACT

New zirconia formulations (4Y and 5Y-zirconias) have been introduced for prosthodontic therapy and are commercialized as "translucent" zirconias. No clinical information providing their survival rates or complications has been provided to the date. This has investigated thesis aimed to investigate different variables regarding some of their mechanical aspects, crystallographic and morphological characterization and alternatives for their cementation.

A finite element analysis was performed in order to observe the stress distribution on a monolithic translucent zirconia crown when cemented with different cements. The bonding potential of a 10-methacryloyloxydecyl dihydrogen phosphate (10-MDP)-based commercial cement to two translucent zirconias was assessed using Raman spectroscopy (RS), Fourier-transform infrared spectroscopy (FTIR) and X-ray photoelectron spectroscopy (XPS). A shear bond strength test was complementary to these analytical methods. The crystallographic structure and surface morphology of two translucent zirconias was estimated by X-ray diffraction (XRD) and interferometry after airborne-particle abrasion (APA) and polishing.
The effect of the cement and air-borne particle abrasion and on the fracture strength of monolithic 4Y-zirconia crowns were also evaluated. And lastly, fracture toughness and hardness were estimated by Vickers hardness measurements.

The stress distribution on a monolithic translucent zirconia crown seems to be unaffected by the cement material. Bonding to 4Y and 5Y-zirconias seems plausible by using a 10-MDP-based cement, nonetheless, thermocycling seems to reduce the bond's strength. The APA protocol produced monoclinic zirconia and was inversely related to the yttria content. Polishing did not cause any monoclinic zirconia. The surface area and surface roughness were increased after the APA protocol. The fracture strength of the monolithic 4Y-zirconias was unaffected by the APA protocol and the cement choice. Differences in fracture toughness and hardness were observed.

Within the limitations of the studies presented in this thesis, it could be summarized that the translucent zirconias differentiate themselves from the traditional formulations, specially 5Y-zirconias in fracture toughness. Special caution is recommended in their clinical use. Nevertheless, bonding seems possible via a 10-MDP based cement.

Keywords: zirconia, translucent, yttria, air-borne particle abrasion, 10-MDP, cement

ISBN 978-91-7833-862-7 (PRINT)
ISBN 978-91-7833-863-4 (PDF)

To the immeasurable value of individual human beings,
with a special dedication to the daily bravery of my beloved Siri,
the courageous wisdom of my mother, Luz Angela,
the unconditional presence of my father, Fabio,
and the outstanding discipline of my brother, Santiago.

"My dear, accept this dedication [. . .] Who you are, I know not; where you are, I know not; what your name is, I know not. Yet you are my hope, my joy, my pride, and my unknown honor."

Søren Kierkegaard
The Crowd is Untruth, *Edifying Discourses in Diverse Spirits*,
Copenhagen, Denmark 1847.

SAMMANFATTNING - SVENSKA

Nya zirkoniamaterial (4Y- och 5Y-zirkonias) har introducerats för protetisk behandling och är marknadsförda som ”translucenta zirkoniamaterial”; emellertid, saknas information gällande materials överlevnad och kliniska komplikationer. Denna avhandling har studerat olika variabler gällande mekaniska aspekter, kristallografiska och morfologiska karakteriseringar och effekten av olika cementval för ett par zirkoniamaterial.

En datorsimulering (finitelementanalys) gjordes för att visualisera spännings-fördelningen hos monolitiska translucenta zirkoniakronor cementerade med olika cementtyper. Bindningspotentialen med ett 10-metakryloyloxydecyl-dihydrogen-fosfat (10-MDP)-baserad cement till 4Y- och 5Y-zirkoniamaterial undersöktes och studerades med hjälp av Raman och Fourier-transform infraröd spektroskopi och röntgenfotoelektronspektroskopi (XPS). Ett skjuvtest (SBS) kompletterade de nämnda analytiska metoderna. Den kristallografiska strukturen och ytmorfologin utvärderades med hjälp av röntgendiffraktion och interferometri efter blästring med aluminapartiklar (Al2O3) och polering. Effekten av cementtyp och blästring på frakturstyrkan av 4Y monolitiska singelkronor utvärderades också. Fraktursegheten och hårdheten beräknades med Vickers hårdhetmätning.

Resultaten visade att spänningsfördelningen i en monolitisk translucent zirkoniakrona är opåverkad av cementmaterialet. Bindning till 4Y- och 5Y-zirkoniamaterial förefaller möjligt med ett 10-MDP-baserad cement, men bindningsstyrkan minskar efter termocykling. Blästring skapade ökad mängd monoklinisk zirkonia och var omvänt relaterad till yttria-innehållet. Polering gav inte upphov till ökad mängd monoklinisk zirkonia. Blästring resulterade i en ökad ytråhet och ytförstoringsgrad, men frakturstyrkan av monolitiska 4Y-zirkoniakronor påverkades inte av cementval eller blästring. Fraktursegheten var omvänt proportionell till yttria-innehållet.

Med hänsyn taget till dessa in vitro-studiers begränsningar kan det ändå konstateras att, de nya translucenta zirkoniamaterialen skiljer sig från de traditionella, speciellt 5Y-zirkoniamaterial i fraktursegheten. Försiktighet rekommenderas i deras klinisk användning. Emellertid, bindning verkar möjligt med ett 10-MDP baserad cement till de translucenta zirkoniamaterialen.

LIST OF STUDIES

The following studies are the structural base of this thesis and are denoted in the text by their Roman numerals.

I. Franco-Tabares S, Stenport VF, Hjalmarsson L, Johansson CB. Limited Effect of Cement Material on Stress Distribution of a Monolithic Translucent Zirconia Crown: A Three-Dimensional Finite Element Analysis. Int J Prosthodont. 2018 Feb;31(1):67–70.

II. Franco-Tabares S, Stenport VF, Hjalmarsson L, Tam PL, Johansson CB. Chemical Bonding to Novel Translucent Zirconias: A Mechanical and Molecular Investigation. J Adhes Dent. 2019;21(2):107–16.

III. Franco-Tabares S, Wardecki D, Nakamura K, Ardalani S, Hjalmarsson L, Stenport VF, Johansson CB. Effect of airborne-particle-abrasion and polishing on novel translucent zirconias: Surface morphology, phase transformation and insights into bonding. In manuscript (Accepted, Journal of Prosthodontic Research, 2020)

IV. Franco-Tabares S, Hjalmarsson L, Kvam K, Johansson CB, Stenport VF. Effect of the cement and airborne particle abrasion on the fracture strength of translucent monolithic zirconia crowns: Remarks on their fracture toughness and hardness. In manuscript (Submitted to the Journal of Prosthetic Dentistry, 2019)

CONTENT

ABBREVIATIONS

Zirconia	Zirconium dioxide (ZrO_2)
3Y	3 molecular percentage (3 mol%) yttria
4Y	4 molecular percentage (4 mol%) yttria
5Y	5 molecular percentage (5 mol%) yttria
Yttria	Yttrium oxide (Y_2O_3)
LTD	Low-temperature degradation
TZP	Tetragonal zirconia polycrystal
PSZ	Partially stabilized zirconia
FSZ	Fully stabilized zirconia
APA	Air-borne particle abrasion
KAPA	Air-borne particle abrasion according to Kern et al: 0.1–0.25 MPa pressure for 15 seconds using 50 μm alumina particles at a distance of 10–12 mm. With a last cleaning step using 99% isopropyl alcohol in ultrasound.
°C	Degrees Celsius
MPa	Megapascals
GPa	Gigapascals
N	Newtons
Å	Ångströms
nm	Nanometres
μm	Micrometres
mm	Millimetres
CAD	Computer assisted design
CAM	Computer assisted manufacture

Alumina	Aluminum oxide (Al_2O_3)
SBS	Shear bond strength
FTIR	Fourier transform infrared spectroscopy
RS	Raman spectroscopy
XPS	X-ray photoelectron spectroscopy
XRD	X-ray diffraction
NMR	Nuclear magnetic resonance
SEM	Scanning electron microscopy
EDX	Energy-dispersive X-ray spectroscopy
eV	Electronvolts
KeV	Kiloelectronvolts
FEA	Finite element analysis
ANOVA	Analysis of variance
.stl	Stereolithography format file
ISO	International standard organization
Vm	Volume fraction of the monoclinic phase in relation to the tetragonal phase.
wt%	Weight percentage

1 INTRODUCTION

Prosthodontics is a discipline of dentistry that is especially concerned with the physical, chemical, and biological properties of dental materials. Typically, this concern is cemented on the premise that "treatment planning, rehabilitation and maintenance" are partially material-dependent, although, the goal of prosthodontic treatment is more or less the same regardless of the materials used: "[to restore] the oral function, comfort, appearance and health of patients with missing teeth and or maxillofacial tissues" (1). In general terms, patients receiving prosthodontic treatment report an improvement in mastication, smile aesthetics, and satisfaction with their mouth (2).

This thesis examines a specific prosthodontic therapy – tooth supported single crowns. This therapy involves "the replacement of missing tooth structure by surrounding the remaining structure by a material" (1). The treatment is multistep, involving the technical expertise of the dentist and the specific knowledge of the dental technician who fabricates the crown for the patient. The treatment ends with the cementation of the crown. A variety of materials – e.g., ceramics, metals, and polymers – are typically used to replace lost tooth structure (1). Similarly, a variety of cements are available to secure the crown onto the remaining dental structure.

In Sweden, single crowns are registered as code 800 (Permanent tooth-supported crown, one per jaw) and code 801 (Permanent tooth-supported crown, many in the same jaw). The latter code incorporates crowns that are units of bridges and therefore are out of the scope of this thesis. Data provided by The Swedish Social Insurance Office (*Försäkringskassan*) shows that during the last four years approximately 190,000 single crowns were cemented every year (Figure 1), with a slight decrease every year. Of these crowns, 30% are registered within the public healthcare system, and the remaining 70% are registered within in private practices (3).

Figure 1. Number of single crowns (code 800) in the last four years in Sweden.

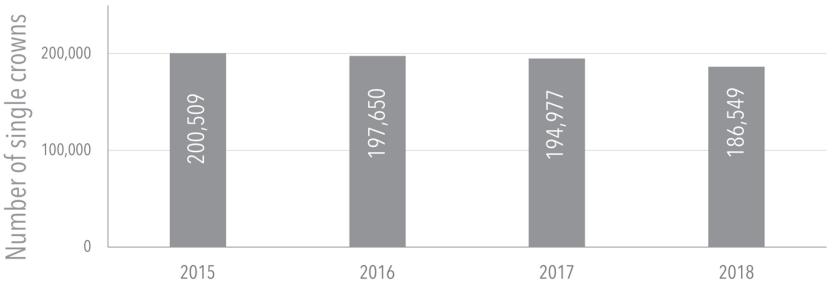

Most of the patients who undergo single crown treatment are between 50 to 79 years old (Figure 2) and are relatively unusual among young adults (20–29 years). As can be observed, single crown treatments are increasingly more common among senior and elderly adults ≥70 years.

Figure 2. Distribution by age (code 800).

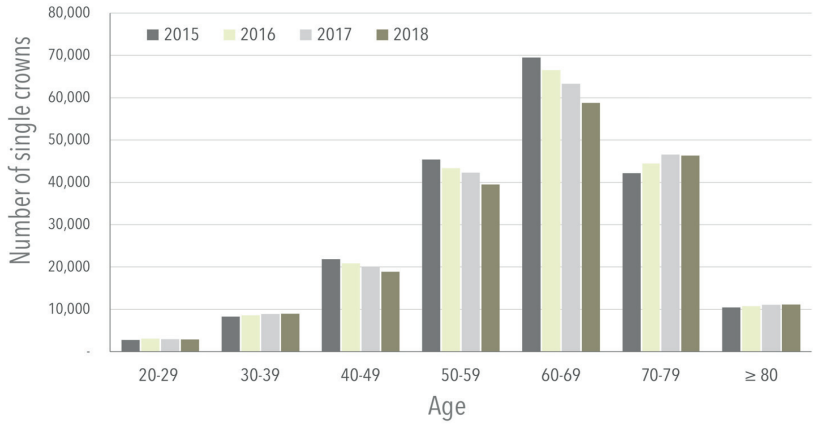

Since 2015, the median price for a single crown has been between 6000 and 6500 Swedish crowns (SEK) (approximately USD 650) in both the public and private sectors. When compared to other dental procedures, single crowns are estimated to be the third most with respect to SEK per year collected: approximately SEK 1,200,000,000 (USD 130 million) are collected per year for single crown treatments (3).

1.1 DENTAL CERAMICS

Ceramics are compounds that consist of a metal/metalloid element and a non-metal element such as oxygen (O). Oxygen, the fuel for most life on this planet, enables, among others, silicon (Si), aluminum (Al), or zirconium (Zr) to become their 'antithesis'. That is, these oxides (silica, alumina, and zirconia) are on the opposite side of the spectrum regarding their physical, chemical, and mechanical properties (4).

Ceramics were adopted in dentistry at the end of the 18th century. The introduction itself into dentistry came with the improvement of the Chinese porcelain recipe (by adding feldspar and decreasing the lime content). This recipe allowed for the production of more translucent porcelains and indirectly dental prostheses. Two Parisian dentists – Nicolas Dubois de Chémant and Guissepeangelo Fonzi – may be responsible for this important step (5).

Dental ceramics are categorized by composition: as particle-filled glasses and polycrystalline ceramics (4). Particle-filled glasses (i.e., glass-ceramics) are amorphous (i.e., non-crystalline). Their main component is feldspathic glass, where the Si-O-Si bond is the most abundant of the amorphous 3D structures (4) (Figure 3). Feldspathic glass includes two important fillers: leucite and lithium disilicate. In a 1962 patent application, leucite was described as the key component for matching the thermal expansion of virtually any dental alloy, making it possible to veneer metal substructures (the invention of metal-ceramic restorations) (6). Lithium disilicate, a more recently introduced filler, improves mechanical properties by reacting when pressed into the feldspathic glass matrix. This mechanism is not new, Dicor (Dentsply, USA), the first all-ceramic material, also used this type of reaction although a different filler (4). In contrast, polycrystalline ceramics have a defined atomic structure. Theoretically, the higher grade of organization represents an increase in mechanical properties but a decrease in translucency by providing light a denser and more arranged medium to pass through (4). Alumina (Al_2O_3) and zirconia (ZrO_2) are the most representative of this group. Alumina and zirconia were used in medical science during the 1970s and late 1980s, respectively, as alternative materials in hip-replacement surgery (7, 8). However, due to their high melting point (>2000 °C), their customization for individual dental restorations was industrially unfeasible. It was not until the CAD/CAM technology

was adopted in dentistry that customized restorations could be made; prior to this, mass production of standardized sizes was used for polycrystalline ceramics.

Figure 3. Illustration of the atomic structure of
a) particle filled-glass ceramic (feldspathic ceramic) (based on (5))
b) polycrystalline (zirconia).

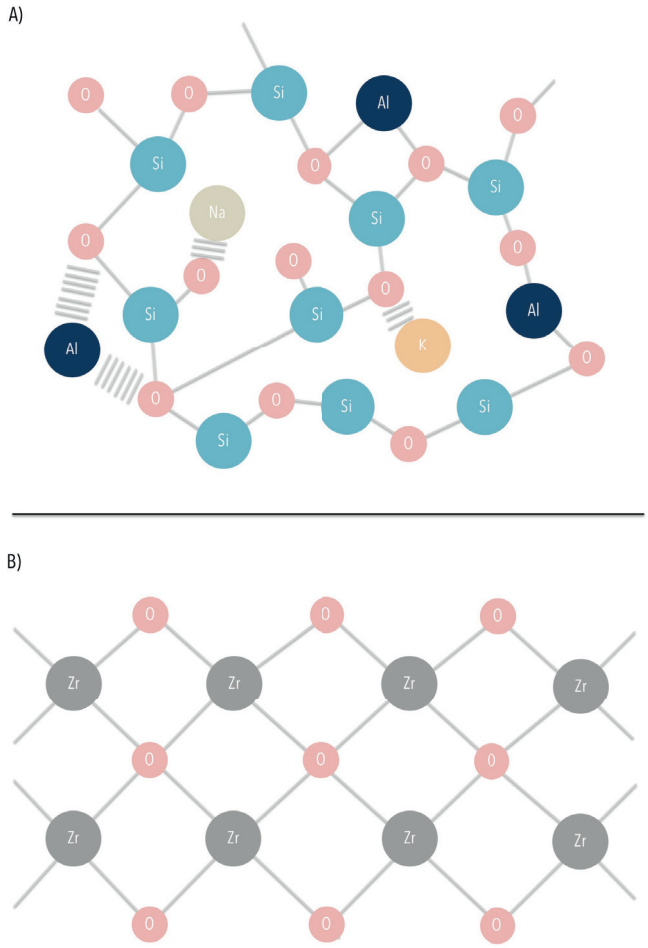

1.2 ZIRCONIA DENTAL CERAMICS

An article published in the journal *Nature*, "Ceramic Steel?", marked the beginning for zirconia ceramics. In this article, Garvie et al. describe "transformation toughening" by making an analogy with a type of steel that undergoes an internal phase transformation that increases its resistance to fracture. In the article, the authors provided experimental data supporting zirconia's phase transformation as a basis for its unusual strength (9).

Zirconia's atoms are organized into three units (i.e., allotropes). They are found at different temperatures in pure zirconia: monoclinic (m) at room temperature, tetragonal (t) at 1170 °C, and cubic (c) above 2370 °C (Figure 4). For each phase, the unit cell volumes are 140 $Å^3$ for monoclinic (10), 68 $Å^3$ for tetragonal, (11) and 138 $Å^3$ for cubic (12). An additional phase has been reported, the rhombohedral. Initially reported by Scott in 1977 (13), later described in ceramic engineering (14–17) and recently reported in dental research literature (18–20). The rhombohedral phase may resemble a symmetrically distorted cube (21). However, unit cell volume estimations are inconsistent. Some authors report it to be 2.5% larger than the cubic unit cell (21) and others 1–2% larger than the tetragonal unit cell (17). However, Scott reported a cell unit volume of 747 $Å^3$ (13). The rhombohedral phase is theorized to be a distorted cubic phase (15,18); however, some studies report the rhombohedral phase to be a distorted tetragonal phase (17,19,20). Moreover, some authors regard the rhombohedral phase as both a distorted tetragonal phase and a cubic phase (14,18). In addition, this rhombohedral phase may be a reorganization of the atoms in the crystal units with the possibility to reverse to tetragonal or cubic after annealing (22).

Different metal oxides have been used to stabilize tetragonal and cubic zirconia at room temperature. Oxides of calcium, magnesium, and cerium are some examples (9,23). However, yttria (Y_2O_3) provides a more effective combination of toughness and strength in relation to the molecular percentage (mol%) used (23). Used at 3 mol%, zirconia constituted mainly by tetragonal units are produced (traditional formulation or 3Y-zirconia) (24).

Figure 4. Zirconia's allotropes

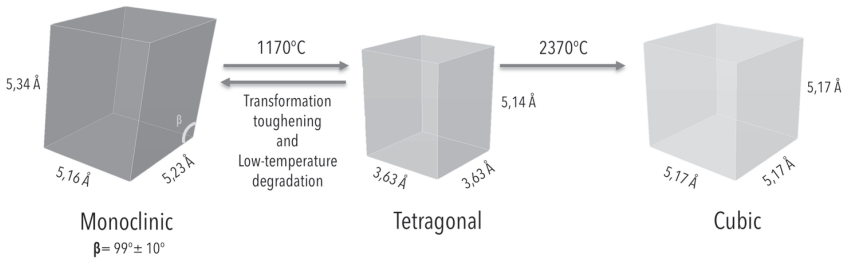

The use of zirconia in dentistry occurred in the early 1990s when it was first used as a filler for porcelain (25). Later in the same decade, zirconia began to be used in ceramic brackets (26) and post systems (27).

As previously mentioned, the progressive adoption and improvement of the CAD/CAM technology facilitated the production of individually customized restorations such as crowns. The first article describing a method to produce monolithic polycrystalline crowns was published in 1999 (28) and the first clinical study, which presented two-year results of the clinical performance of zirconia-based crowns, was published in 2009 (29).

1.2.1 Translucent zirconias

The opacity of zirconia compared to glass-ceramics or natural teeth is a shortcoming when used as monolithic material (30). It has been reported that the phenomenon behind this may be two-fold: a) the presence of pores, defects, and light-scattering dopants and b) zirconia-specific light-scattering (30).

Yamashita and Tsukuma reported that pore size and porosity significantly affect the translucency of yttria stabilized zirconia (31). A porosity of 0.1% with a pore diameter of 100 nm decreases the translucency to 0% at a thickness of 1 mm (31). However, other authors have documented that at a porosity of 0.01% translucency can still be achieved at 1-mm thickness even if the pore size is greater than 100 nm (32). Alumina has been used as a dopant for zirconia ceramics given its capacity to increase the final density (33). When used at >0.1 mass%, densities approaching the theoretical maximum are reached at a sintering temperature of 1300 °C (33). Nevertheless, the refraction index of alumina differs compared to the refraction index of zirconia (34). Zhang et al. showed that alumina-doped 3Y-zirconia presents three times more light scattering than alumina-free 3Y-zirconia (34).

The presence of various phases in zirconia ceramics gives rise to the second obstacle regarding the opacity of zirconia-based restorations. The tetragonal and the cubic phases have different refraction indexes, making the ceramic birefringent or optically anisotropic (32,35,36). The refraction index is a comparison of the speed of light travelling though air with the speed of light travelling through a material. The cubic phase has a refraction index of 2.16 and the tetragonal phase has a refraction index of 2.20 (36). Additionally, the refraction index for zirconia is higher compared to that for other ceramic systems. Refractive indexes reported in the literature are 2.20 for zirconia (30), 1.76 for alumina (30), 1.51 for leucite (37), and 1.50 for feldspathic glass (dental porcelain) (38). Summarizing, light travels 2.16-2.20 times slower when passing through zirconia than when passing through air.

Different approaches have been proposed to solve the opacity problem of zirconia. For example, Zhang modeled a theoretical minimum grain size to produce translucent 3Y-zirconia (30). Using a Rayleigh scattering model, the author recommends a maximum grain

size of 82 nm to produce the same translucency as dental porcelains at a thickness of 1.3 mm (30). Other authors propose inclusion of large cation radius dopants such as La_2O_3 and Nd_2O_3 in traditional formulations (39,40). The addition of those oversized dopants is suggested to improve the translucency of traditional formulations up to 42% of their initial translucency (40). These dopants, used at 0.2% mass, seem to be localized at the outermost region of the grain boundaries. The mechanism may be a reduction in the birefringence of zirconia by grain boundary segregation (40).

Increasing the content of yttria in terms of mol% has been another alternative (30). Increasing the mol% of yttria up to 4 to 5% is the basis for materials that today are commercially available as "translucent zirconias" (4Y- and 5Y-zirconias) (41). Although originally used as a marketing term for zirconia, today "translucent" is used to describe all types of zirconias, from traditional formulations to the new 4Y and 5Y formulations (41). However, the new formulations, specifically the 5Y-zirconia, report half of the flexural strength and more than half of the fracture toughness of the traditional formulations (41).

1.2.2 Mechanical and optical properties

Zirconia ceramics report a superior flexural strength and fracture toughness compared to other ceramic systems, especially the traditional formulations compared to glass-ceramics. The flexural strength of traditional formulations is $\geq$ 900 MPa, which could be illustrated as follows: fracture at flexure occurs when a 90-kg rugby player "stands" on a square millimeter. This flexural strength is, for example, 10 times higher than the first all-ceramic material (Dicor, Dentsply, USA) (42) and double as much as the flexural strength of lithium disilicate (43). Fracture toughness, refers to the material's ability to resist fracture provided a preexisting defect. Reported fracture toughness values for yttria stabilized zirconia seem to be inversely proportional to the yttria content (44). For traditional formulations, values are around 5 $MPa.m^{1/2}$, which is approximately 1.5 times higher than those of lithium disilicate (45). The elastic-modulus, however, has been observed to be constant (210 GPa). Traditional formulations, which are predominately tetragonal, present the same elastic modulus as 100% cubic formulations (46,47).

Transformation toughening is the mechanism responsible for these mechanical properties (44,48) (Figure 5). The phase transformation from tetragonal to monoclinic phase involves a shear strain of 8% and a volume expansion of 4% (44). This phenomenon results in the arrest of fractures and flaws, stopping their propagation within the material (44). For 4Y- and 5Y-zirconias a decrease in their flexural strength and fracture toughness is reported (45,49); however, limited literature addresses this topic.

Figure 5. Transformation toughening.

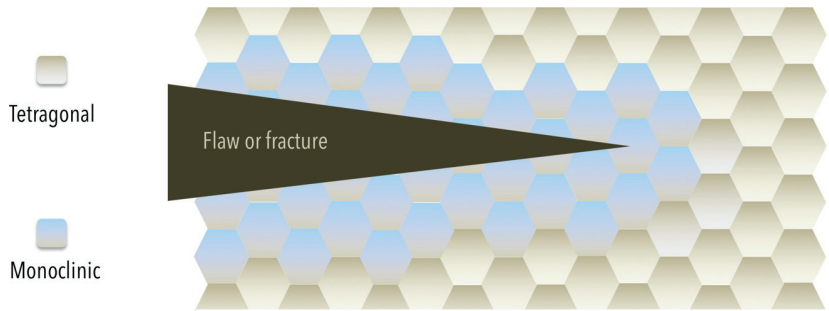

Zirconia's birefringence and high refraction index results in typical low translucency values compared to other ceramic systems, as previously mentioned. Traditional formulations report translucencies at 1.0-mm thickness of 20%, 5Y-zirconia of 23%, and lithium disilicate of 27% (50). At a reduced thickness of 0.5 mm, traditional formulations have a translucency of 28% and 5Y-zirconia has a translucency of 32%, both contrasting with lithium disilicate's translucency of 40% at the same thickness (50).

Grain size is related to both optical and mechanical properties of zirconia. For traditional formulations, an increase in grain size is related to a decrease in mechanical properties (51) and translucency (30). However, 5Y-zirconia formulations show variability in grain size (350 nm to 810 nm) (49) but still exhibit an increased translucency (50).

1.2.3 Chemical and biological properties

A particular phenomenon occurs in zirconia ceramics, especially the traditional formulations with high tetragonal content. Given that a stabilizer (i.e., yttria) is used to produce tetragonal units at room temperature, the ceramic itself is called "metastable" as the ceramic can phase transform in a defined setting. When this transformation occurs related to temperature, the phenomenon is termed low-temperature degradation (LTD).

Kobayashi et al. found that zirconia formulations containing 4.5 to 5 mol% yttria could present approximately 20% monoclinic content after 3000 hours at 200–300 °C (52). Nevertheless, formulations containing more or equal than 5% and up to 8.0% mol yttria reported 3 to 0% monoclinic content after ageing at the same temperature and for the same period (52). The temperature interval at which this phenomenon happened most rapidly was believed to be a limiting factor with respect to clinical use. In 2001, a certain amount of zirconia-based hip prosthesis started to present catastrophic failure (fracture of the prosthesis). Reports investigating the failed prostheses showed an increased surface roughening and monoclinic phase content after clinical service for as short as 1–2 years (53,54) (Figure 6). Further investigations showed that a certain batch of zirconia hip heads underwent an alternative sintering protocol (23). This alternative method used a cooling protocol twice as rapid together with the use of a tunnel furnace instead of a closed furnace and slow cooling. The consequences of this faster sintering protocol may have resulted in increased porosities of the zirconia hip heads. An increased porosity or a decreased density probably was the determining factor that lead to an accelerated LTD (24).

An additional factor associated to LTD is grain size. An increased grain size has been correlated to an increased LTD (55). It is theorized that larger grains are enriched with the predominantly cubic stabilizer, yttria. Other regions, specifically yttria-deficient regions, are destabilized tetragonal regions and more susceptible to LTD (55). Nevertheless, LTD is not an exclusive problem of zirconia with lower density or with increased grain size. It has been shown that a certain amount of LTD is expected to occur in optimally-sintered traditional zirconias (24). In response to these issues, the International Standard Organization presented a regulation (ISO 13356) specifying, among

others, a minimum density (≥ 6.0 g/cm^3) and grain size (≤ 400 nm) for yttria stabilized zirconia surgical implants.

The new formulations of zirconia are yet to be investigated in this matter. Theoretically, a factor that could be favorable is the increased amount of cubic zirconia that cannot transform to tetragonal and then to monoclinic. Nevertheless, the mechanical properties may be a shortcoming, and for some formulations the larger grain size may be a shortcoming (51).

Figure 6. Low-temperature degradation.

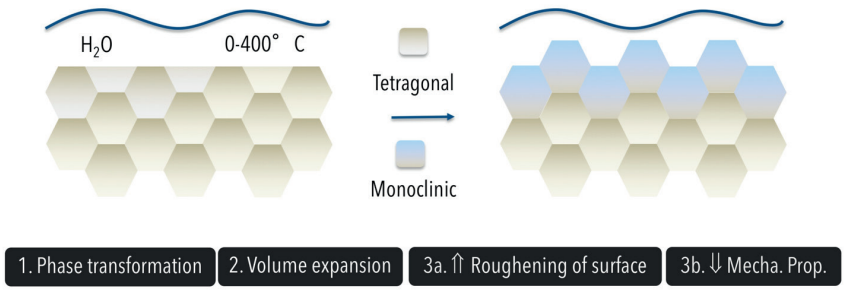

The effect of air-borne particle abrasion (APA) in relation to low-temperature degradation has been documented. Cotic et al. reported that a traditional formulation sintered at 1500 °C that underwent APA with 50-μm and 110-μm alumina particles at 0.25 MPa results in a decreased formation of monoclinic content (40% less) compared to as-sintered specimens after artificial ageing in an autoclave at 137 °C for 12 and 48 hours (56). Other studies have noted this phenomenon in traditional formulations and have observed that for traditional formulations APA provides a form of protection against LTD (20,57). However, the mechanism is not fully understood (20), and translucent formulations need further exploration.

Studies of zirconia-based materials have reported favorable results in terms of biological properties. Variables aiming to measure osseointegration, such as bone-implant contact and peri-implant bone volume density, are reported to be at least as much as the ones observed for titanium in a variety of animal models (white rabbits, mini-pigs, adult pigs, and beagles) for 2 to 12 weeks (58–63). Clinical studies including zirconia abutments in peri-implant soft tissue conditions have not reported any significant differences compared to

titanium abutments in terms of variables such as plaque index, gingival index, and periodontal probe depth (64–67). Other clinical studies measuring bacterial adhesion using variables such as bacterial count and area colonized have not documented any statistical differences between titanium and zirconia abutments (68–70). It has been theorized that the biological inherent properties of zirconia may not interfere in the normal proliferation of fibroblasts, which facilitates the structuring of a good mucosal barrier (71). Because the mentioned clinical studies are short; long-term clinical trials are needed before any valid recommendation can be made. Furthermore, the new formulations of zirconia have not been investigated regarding their potential osseointegration, peri-implant soft tissue reaction, and bacterial colonization.

1.3 DENTAL CEMENTS

Dental cements are used in the last step of single crown treatment. Their main function is to firmly unite the crown with the tooth preparation, which is ultimately the patient. Cements have been present in the daily clinical practice since the use of zinc phosphate at the end of the 19th century (Figure 7) (72). Other cements were gradually introduced into dentistry, specifically with the advancement of polymer and glass technologies. The resin-based cements were introduced at the beginning of the 1960s (73), the glass-ionomers in the mid 1970s (74), and the resin-modified glass-ionomers in the early 1990s (75).

Figure 7. An 1892 report on using zinc phosphate as cement.

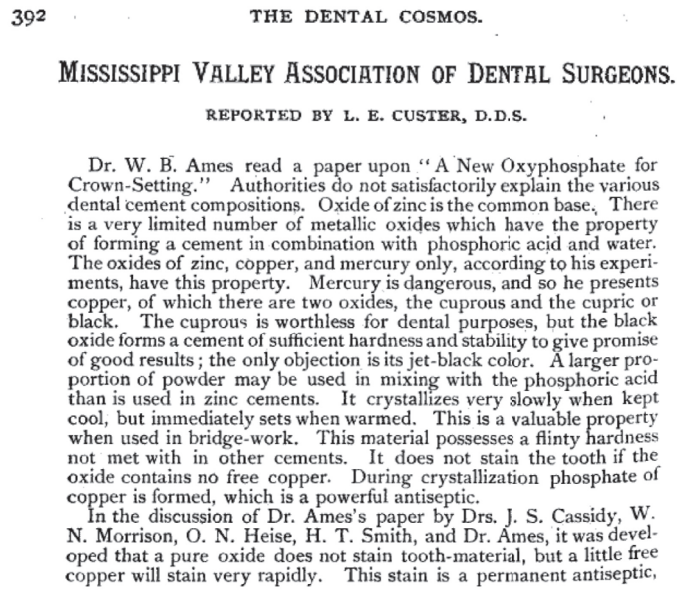

392 THE DENTAL COSMOS.

MISSISSIPPI VALLEY ASSOCIATION OF DENTAL SURGEONS.

REPORTED BY L. E. CUSTER, D.D.S.

Dr. W. B. Ames read a paper upon "A New Oxyphosphate for Crown-Setting." Authorities do not satisfactorily explain the various dental cement compositions. Oxide of zinc is the common base. There is a very limited number of metallic oxides which have the property of forming a cement in combination with phosphoric acid and water. The oxides of zinc, copper, and mercury only, according to his experiments, have this property. Mercury is dangerous, and so he presents copper, of which there are two oxides, the cuprous and the cupric or black. The cuprous is worthless for dental purposes, but the black oxide forms a cement of sufficient hardness and stability to give promise of good results; the only objection is its jet-black color. A larger proportion of powder may be used in mixing with the phosphoric acid than is used in zinc cements. It crystallizes very slowly when kept cool, but immediately sets when warmed. This is a valuable property when used in bridge-work. This material possesses a flinty hardness not met with in other cements. It does not stain the tooth if the oxide contains no free copper. During crystallization phosphate of copper is formed, which is a powerful antiseptic.

In the discussion of Dr. Ames's paper by Drs. J. S. Cassidy, W. N. Morrison, O. N. Heise, H. T. Smith, and Dr. Ames, it was developed that a pure oxide does not stain tooth-material, but a little free copper will stain very rapidly. This stain is a permanent antiseptic,

Dental cements are categorized into two large groups: water-based and resin-based. The International Standard Organization has separate documents regulating each group (ISO 9917 and ISO 4049, respectively). The water-based cements are set using an acid-base reaction, and the resin-based cements react by polymerization.

Special interest on the properties of various dental cements has existed since they are the linking agent between the restoration and the patient. The cements have also been considered as a potential vehicle for delivering fluoride, for example, adhering chemically to

the dental structure and restoration, stimulating the formation of reparative dentin and impeding the colonization and sometimes re-colonization of the remaining dental structure by bacteria (76).

Some minimum values for compressive and flexural strength have been recommended by the International Standard Organization (Table 1). Compressive strength seems to be of special interest for water-based cements and flexural strength seems to be of special interest for resin-based cements. The standards (9917-1:2007, 9917-2:2017 and 4049:2019), however, do not explain how these minimum values can be related to clinical success or at least related to clinical studies.

Table 1. Compressive strength and flexural strength of the most representative cements.

Cement	Compressive Strength	ISO requirement	Flexural Strength	ISO requirement
Zinc phosphate	69 MPa	50 MPa (9917-1:2007)	6 MPa	Not specified
Glass-ionomer	104 MPa	50 MPa (9917-1:2007)	15 MPa	Not specified
Resin-modified glass-ionomer	115 MPa	Not specified	15 MPa	10 MPa (9917-2:2017)
Resin	166 MPa	Not specified	90 MPa	50 MPa (4049:2019)

Values obtained from (77)

The biological properties of dental cements are of particular interest given their close proximity to the dentino-pulpal organ and the gingiva. Different cellular models have presented varying results (76). Zinc phosphate results in a higher human gingival fibroblast viability than glass-ionomer and resin cement (78). However, contrasting results exist regarding rat fibroblasts (79). It is speculated that the determining factor could be the remaining substances produced by the reaction or un-reacted material irrespective of cement (76,78). Allergic reactions to dental cements have been reported, mostly to resin-based cements, but these reactions are rare (80,81).

The bonding capacity of dental cements has also received special attention. Cements containing functional groups that can theoretically bond to the dental structure or to a variety of materials have been developed.

Polyacrylic acid (PAA), present in glass-ionomers, is believed to bond with the hydroxyapatite existing in dentin and enamel (82). The carboxyl functional group (COO^-) seems to form an ionic bond with the hydroxyapatite's calcium (Ca) and is resistant to ultrasound (82). Other molecules present in resin adhesives – e.g., 4-methacryloxyethyl trimellitic acid (4-MET), 2-methacryloxyethyl phenyl hydrogen phosphate (phenyl-P), and 10-methacryloyloxydecyl dihydrogen phosphate (10-MDP) – can bond to the calcium present in hydroxyapatite (83). Bonding to glass-ceramics, for example, is based on the same principle as the bonding of the silica filler particles to the polymer matrix of common dental composites. A silane is applied as the coupling agent between the cement and the glass-ceramic (84).

1.4 ZIRCONIA SINGLE CROWNS

The estimated five-year survival rate of zirconia single crowns is 93.8%, a survival rate statistically equal with metal ceramic single crowns. The two main complications are porcelain chipping (approx. 3%) and loss of retention (approx. 4%) (90). Chipping of the veneering porcelain was a recurrent clinical problem for zirconia-based restorations at the beginning of the last decade (85). Different theories were presented to explain this phenomenon (5): mismatch of the thermal expansion of zirconia and porcelain, for example, or phase transformation from tetragonal to monoclinic at the zirconia-porcelain interface (86). However, these clinical problems appear to be the result of residual stresses accumulated during rapid cooling of the veneering porcelain (85). After a slower cooling protocol was adopted, especially during the last porcelain firing, a decrease in chipping has been reported (5). Given this complication, monolithic zirconia restorations are an alternative to veneered zirconia.

1.4.1 Effect of the cement

The effect of the cement on the fracture strength of monolithic traditional zirconia single crowns seems to be negligible. Nakamura et al. documented that monolithic 3Y-zirconia single crowns had no statistical different fracture strength when cemented with zinc phosphate, glass-ionomer, and a resin cement, even at a reduced thickness of 0.5 mm (87). The effect of the cement in the fracture strength of 4Y and 5Y formulations has not been investigated. Clinical literature concerning this apparent versatility of veneered 3Y-zirconia can be found in Table 2 (88–97). Two studies reported loss of retention. Örtorp et al. reported loss of retention of 15 crowns with both cements – zinc phosphate (n=2) and resin cement (n=13) (91). Monaco et al. registered two crowns losing retention that were cemented with resin cements (94). The American Academy of Prosthodontics has also registered this apparent versatility (98). Nonetheless, long-term studies that include both water-based and resin-based cements are still needed to provide a better understanding of the topic (98).

Table 2. Cements used for traditional zirconia-based single crowns.

Year/Authors/Country/Type of Study, mean follow-up time	Cements used, n=number of crowns
2017/Dogan et al./USA Prospective, 49 months	Dual-cure self-adhesive resin-cement (RelyX Unicem, 3M, USA), n=20
2015/Seydler and Schmitter/ Germany Randomized controlled trial, 25 months	Self-curing resin-cement (Multilink Automix, Ivoclar Vivadent, Liechtenstein), n=30
2014/Gherlone et al./Italy Retrospective, 36 months	Dual-cure self-adhesive resin-cement (RelyX Unicem, 3M, USA), n=86
2013/Monaco et al./Italy Retrospective, 60 months	Resin cement, n=792 Glass-ionomer, n=235 Zinc-phosphate, n=77
2013/Rinke et al./Germany Prospective, 36 months	Resin-modified glass-ionomer (Dyract Cem plus, DeTrey, USA), n=52
2012/Sagirkaya et al./Turkey Randomized controlled trial, 74 months	Dual-cure self-adhesive resin-cement (Panavia f2.0, Kuraray, Japan), n=74
2012/Örtorp et al./Sweden Retrospective, 60 months	Zinc phosphate (Phosphacem, Ivoclar Vivadent, Liechtenstein), n=16 Self-adhesive resin-cement (Rely X Unicem, 3M, USA), n=200
2012/Vigolo et al./Italy Prospective, 48 months	Glass-Ionomer (Ketac-Cem, 3M, USA), n=39
2010/Beuer et al./Germany Prospective, 35 months	Glass-Ionomer (Ketac-Cem, 3M, USA), n=50
2010/Schmitt et al./Germany Prospective, 39 months	Glass-Ionomer (Ketac-Cem, 3M, USA), n=17

1.4.2 Bonding to zirconia

There is an interest in creating a stable chemical bond to zirconia that resembles the stable chemical bond for glass-ceramics. The possibility of combining the advantageous mechanical properties of zirconia with a bonding protocol is appealing, especially in the age of minimally invasive dentistry. Moreover, this development could address the main clinical complication – loss of retention. Due to the nature of zirconia, the same protocol of acid etching with hydrofluoric acid (HF) at room temperature and silanization cannot be performed (84). More than 20 methods to create a bond to zirconia (e.g., the use of laser treatments, glass infiltrations, and primers) have been explored (99).

The molecule 10-MDP, designed to have hydrophilic and hydrophobic properties (amphipathic), was initially engineered for dentinal bonding but later investigated as a potential bonding molecule to multiple materials (100). Suzkuki et al., using vibrational spectroscopy, have provided molecular evidence that 10-MDP bonds to silver (Ag) and this bond is stable up to 200 thermocycles (101). Moreover, the stability of the bond seems to be improved compared to a similar molecule but shorter in nature (2-MDP) (101). Similar findings using vibrational spectroscopy regarding molecular bonding of 10-MDP to chrome (Cr) have also been documented (102).

The possibility of bonding to different substrates means that 10-MDP is categorized as an universal adhesive (103). More recently, the potential bonding of 10-MDP to zirconia has been investigated. Chen et al. provided molecular documentation of the possible bond Zr-O-P using time-of-flight secondary ion mass spectrometry (TOF-SIMS). Other studies using Fourier-transform infrared spectroscopy (FTIR) reported the adsorption of 10-MDP on traditional zirconia formulations (104–107). The above studies registered peaks at 1083 and 981 cm^{-1}, which were assigned to the asymmetrical and symmetrical vibrations of the PO_3^{2-} functional group from 10-MDP adsorbed on traditional zirconia (104–107). Another analytical method that has been used to assess the bond of 10-MDP to traditional zirconia has been X-ray photoelectron spectroscopy (XPS) (106–108). The principal focus of the mentioned studies has been the analysis of the intermediate oxygen present in the Zr-O-P bond and specifically its first level of energy (Os1) (106–

108). Energies corresponding to that possible bond have been shown to exist in the 531.5–531.8 eV interval (109).

Using nuclear magnetic resonance (NMR), some studies have provided insight into how 10-MDP may be adsorbed onto traditional zirconia by the interaction between the P-OH and Zr-OH groups or between P-O^- and partially positive Zr^{4+}. Moreover, the Zr-O-P bond is resistant to ultrasound when exposed to acetone for 40 min, and being possibly an ionic bond (110). The modification of 10-MDP for improving its affinity to zirconia has also been explored (106). Using acetone or ethanol as solvents may provide a better affinity compared to using water (106). Moreover, if the carbon chain is extended over 10 carbons with the inclusion of a carboxyl (COO^-) or a hydroxyl (OH^-) group in the middle of the chain, unlike a typical 10-MDP molecule used in traditional zirconia, affinity may be improved (106).

Indirect methods such as mechanical testing have also been used. Shear bond strengths seem to range between 10–20 MPa (108,111), and tensile bond strengths seem to range between 30–50 MPa (112).

Figure 8. a) the 10-MDP molecule and b) the cations for bonding.

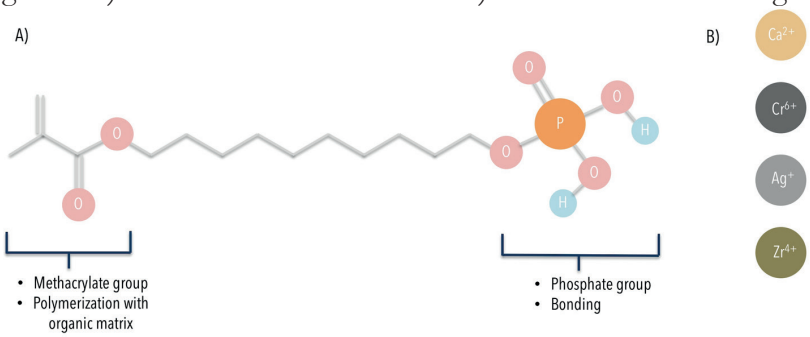

Clinical studies involving 10-MDP have been presented by a research group led by Professor Matthias Kern from the University of Kiel. The group developed a procedure that involves the air-particle abrasion of the surface at 0.1–0.25 MPa for 15 seconds using 50-µm alumina particles at a distance of 10–12 mm. The last cleaning step uses 99% isopropyl alcohol in an ultrasound cleaner. Subsequently, a 10-MDP-based cement or primer is used. To date, two clinical studies have investigated clinical outcomes: a ten-year retrospective study evaluating the survival rate of zirconia-based cantilever resin bonded fixed dental prostheses (RBFDPs) in the anterior region (113) and a three-year prospective study reporting the survival rate of zirconia-

based inlay-retained fixed dental prostheses (IRFDPs) in the posterior region (114). The anterior region had a survival rate of 98.2% after ten years and the posterior region had a survival rate of 100% after three years. However, the anterior region study had a retrospective design, the posterior region study had a small sample size (n=23) for the three-year follow-up, and both studies did not include a control group. Additionally, other research groups need to confirm the clinical outcomes independently. Moreover, no information has been reported that describes how to use this protocol to bond translucent zirconias.

2 AIM

This thesis investigated some mechanical aspects, phase transformation, and cement considerations for 4Y- and 5Y-zirconias.

The specific aims of this thesis were as follows:

a. To evaluate the effect of various cements on the stress distribution of a monolithic translucent zirconia crown.

b. To study the bonding potential of a 10-MDP-based cement for two translucent zirconias.

c. To assess the effect of an air-particle abrasion protocol and polishing on two translucent zirconias.

d. To observe the effect of an air-particle abrasion protocol and cement on the fracture strength of 4Y-zirconia monolithic crowns.

3 MATERIALS AND METHODS

Zirconias used in this thesis

Three types of zirconias were used in this thesis. They were differentiated from each other by the flexural strength provided by each manufacturer.

Table 3. Trade name, lot number, flexural strength, and manufacturer of the different zirconias used in this thesis.

Trade name	Provided Flexural Strength	Manufacturer
BruxZir 2.0 HT (lot B1226355)	>800 MPa	Glidewell, USA
DDcubeX^2 HS (lot 6161719002)	1100 MPa	DentalDirekt, Germany
Copra Smile (lot IS2189A2)	600 MPa	Whitepeaks, Germany

The materials were elementally characterized by energy dispersive X-ray spectroscopy (EDX). One block (3 mm x 3mm x 1mm) of each zirconia was embedded in epoxy resin (EpoFix batch 4138-3380, Struers, Denmark) to facilitate its handling and polishing. The polishing procedure was carried out with SiC papers (Struers, Denmark) (#500, #1000, #1200, #2400, and #4000) until optical finish. Following extensive water rinsing and drying, the three specimens were mounted on aluminum stubs using carbon tape. The elemental information was gathered from five points per specimen and can be found in Table 4.

Varying mean values of yttrium were observed (Table 4). Estimations of the yttria (Y_2O_3) molecular percentage (mol%) were 2.7 mol% for BruxZir 2.0 HT, 4.2 mol% for DD cubeX^2 HS, and 4.8 mol% for Copra Smile. However, these values are most likely approximations given the low electrical conductivity of the specimens and the similar values for the yttrium and zirconium Lα spectral lines (1.924 and 2.044 KeV respectively) (115). This can be observed from the broad peak initiating from 1.9 to 2.3 KeV (Figure 9). Consequently, the materials were assumed to be 3, 4, and 5 mol% yttria stabilized zirconia – BruxZir 2.0 HT, DD cubeX^2 HS, and Copra Smile, respectively.

Table 4. Elemental characterization of the zirconias used in this thesis.

	Atomic % (SD)		
	O	Zr	Y
BruxZir 2.0 HT	67.6% (0.4)	30.7% (0.3)	1.7% (0.1)
DD cubeX^2 HS	67.4% (0.3)	30.0% (0.2)	2.6% (0.1)
Copra Smile	67.4% (0.6)	29.7% (0.5)	3.0% (0.1)

SD: Standard deviation

Figure 9. EDX spectra of the three zirconias: a) BruxZir 2.0 HT; b) DD cubeX^2 HS; and c) Copra Smile.

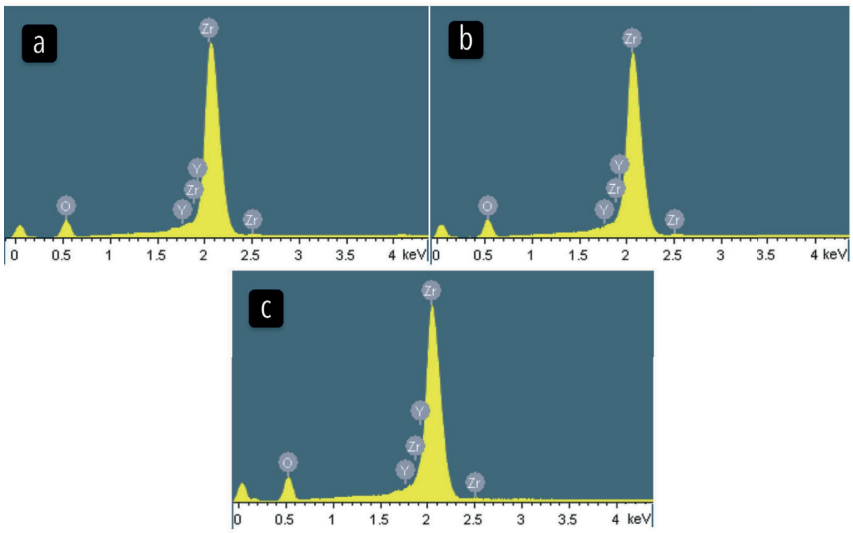

3.1.1 Mechanical analyses

Finite element analysis (Study I)

A standard lower molar gypsum die (Fujirock, GC, Japan) was prepared for a single crown using a high-speed handpiece (Ti95, NSK, Japan). The taper of the preparation was measured with a Nikon SMZ800 stereomicroscope (Nikon Instruments, USA), and the image software analysis (NIS-Elements BR 3.2, Nikon Instruments, USA) was performed using a total magnification of 10×. A total of four angles on four surfaces were measured (buccal, lingual, mesial, and distal). The reference point for each angle was 1.0 mm above the finish line as previously described (116). The total occlusal convergence angles were 14° buccolingually and 17° mesiodistally, which are both within the ranges previously recommended to obtain a proper retention and resistance (117,118). Both the preparation and the full anatomic crown were scanned using a laser scanner (3Shape D700, 3Shape A/S, Denmark). Both the marginal gap (MG) and the cement thickness (CT) were modelled based on information provided by clinical findings (119,120). The MG was modelled as 110 μm, and the CT was modelled as 280 μm on the occlusal surface and 110 μm on the axial walls. The thickness of the crown at the central fossa was 1.0-mm and 0.5-mm thick peripherally on the cervical margin. The loading force magnitudes (225 N and 600 N) and their directions (0° and 19.5°) were obtained from clinical findings (119–122). The number of loading points was described using two conditions: a conventional cusp-to-marginal ridge occlusion resulting in five points and one single loading point in the central fossa. The diameter of the loading points (ø 1.25 mm) was also obtained from the literature (123).

A variety of cements were evaluated: zinc phosphate, glass-ionomer, resin-modified glass-ionomer, dual-cure resin, calcium aluminate-based, and a theoretical or conceptual cement. The latter was intended to represent a cement with mechanical properties resembling dentin. As the information regarding the mechanical properties of the periodontal ligament was inconclusive, this information was omitted. The proportional limit of each material was selected as the failure parameter because a plastic deformation for the brittle materials used in the present study simply represents a fracture

of the material itself (77). For the cements, the proportional limit values were obtained from a reference (77). The calcium aluminate-based cement was provided by the manufacturing company (Doxa AB, Sweden). Information about dentin was obtained from the literature (42). For the monolithic translucent zirconia crown, an average value (1000 MPa) for the flexural strength of various commercially available translucent zirconias was used.

Figure 10. Loading conditions. Every loading condition is a combination of three variables: loading force, angle, and number of contact points.

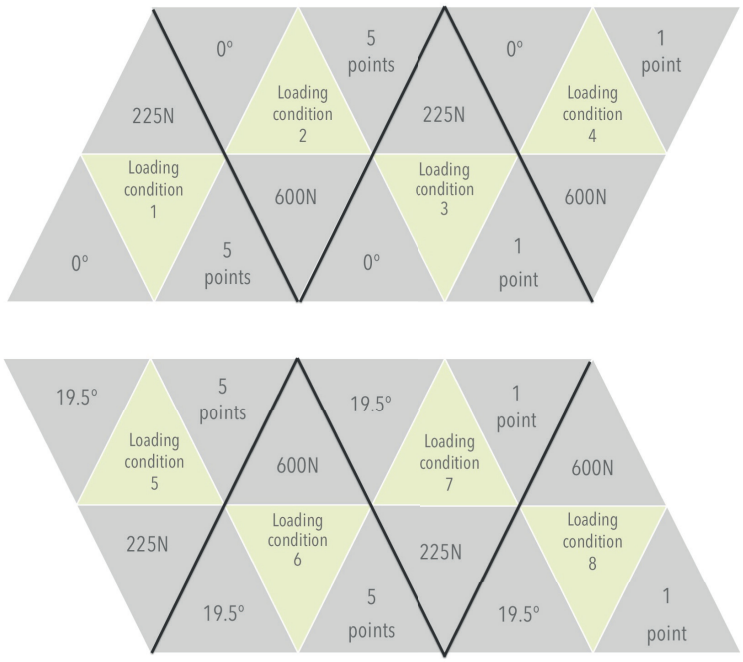

At the bottom of the abutment, a flat surface parallel to the occlusal plane of the crown was set as a fixed support. No sliding or separation was allowed between the interfaces of the components (crown-cement abutment). The software used to model the CT was Dental System 2014™ premium (3Shape A/S, Denmark) and Autodesk 3ds Max 2011 (Autodesk Inc., USA). The average element quality was 0.82 (SD 0.09): 1 was the highest and 0 the lowest quality according to the simulation software (ANSYS Workbench 2015, SAS IP Inc., USA).

In total, the model included 525,734 tetrahedral elements, 829,647 nodes, and 2,488,941 degrees of freedom (three degrees of freedom per node). The total number of simulations was 48 (8 per cement).

Table 5. Elastic modulus and Poisson's ratio of the materials used.

Material	Elastic Modulus, GPa	Poisson's ratio, unitless
Dentin	19 (124)	0.30 (124)
Conceptual cement	18	0.30
Zinc phosphate	13,5 (42)	0.33 (125)
Glass ionomer	7,3 (42)	0.35 (126)
Resin modified glass ionomer	5,1 (42)	0.30 (127)
Calcium aluminate-based	4,5 *	0.28 *
Dual cure resin	6,5 (128)	0.30 (129)
Zirconia	210 (47)	0.30 (42)

*Information provided by Doxa AB, Sweden.

Shear bond strength (Study II and Study III)

Studies II and III included a shear bond strength (SBS) test based on the ISO standard 29022:2013 (Figure 11). The standard uses a notched-edge stylus designed to homogenously distribute the stress generated at the interface of the adhered materials. The specimens (n=10) were cylinders (3.0 mm ⌀ x 2.0 mm height) of each type of zirconia produced according to the manufacturers' instructions. The specimens were embedded in epoxy resin (EpoFix, batch 4138-3380 for Study I and batch 8348-01 for Study II, Struers, Denmark) and polished until the zirconia surface was exposed. The polishing process was carried out using SiC papers (Struers, Denmark) until optical finish, in Study II #500, #1000, #2000 and #2400. In Study III until #4000 with final polishing step using a polishing cloth moistened with a lubricant (DP-Lubricant Blue, batch 5335, Struers, Denmark) and a polishing suspension (OP-S Suspension, batch 4218-8333, Struers, Denmark). After polishing, the specimens were cleaned from any residual polishing particles by ultrasound for 20 minutes

and rubbed with 99% isopropyl alcohol for three to four seconds. The specimens were left to dry at room temperature.

In Study II, air particle abrasion of the surface was performed according to Kern's protocol (KAPA) (0.1–0.25 MPa, 50-μm alumina, 10–12 mm distance, 15 seconds, and cleaning in ultrasound using 99% isopropyl alcohol). In Study III, a first SBS test was performed using the highly polished surface. Composite cylinders of 2.4 mm ⌀ x 1.5 mm height were used in Study II and III (Spectrum TPH3 lot 1707000722 for Study II and lot 0986 for Study III) (Dentsply Sirona, USA). In Study III, for the second SBS test, the surface was cleaned with ultrasound for 15 minutes. After the cleaning procedure, they underwent KAPA, and the second SBS test was carried out. Zinc phosphate cylinders (2.4 mm ⌀ x 1.5 mm height) were used (liquid, normal setting lot 1101609; powder, normal setting lot 91605022) (Harvard Dental International, Germany). For the manufacture of all the cylinders, a poly methyl methacrylate (PMMA) (White Peaks, Germany) mold was used. For the composite cylinders, a 10-MDP-based cement was used (Panavia F 2.0, lot 000055 both pastes in Study II and Paste A lot 7E0167, Paste B lot 270072 in Study III) (Kuraray, Japan). For the zinc phosphate cylinders, the same zinc phosphate cement was used. The manufacturer's recommendations were followed. Following the ISO standard 29022:2013, the specimens were stored in deionized water at 37 °C for 24 hours. In Study II, half of the specimens were thermocycled 10,000 times (5 °C–55 °C). Next, the specimens were mounted in a universal testing machine (LRX 9772, Lloyd Instruments, UK). A notched-edge cross head at a rate of 1.0 mm/min was used. The shear bond strength was calculated by dividing the force at de-bonding (N) by the bonding area (≈4.52 mm^2).

Figure 11. Illustration of the specimens for the shear bond test.

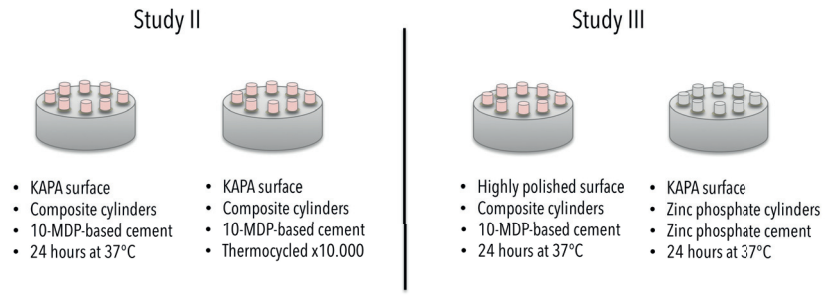

Fracture strength (Study IV)

The digital models (.stl format) of the crown and abutment from the finite element analysis were used. The monolithic crowns were manufactured from DD cubeX^2 HS (DentalDirekt, Germany) zirconia and the abutments from G10, a glass-epoxy laminate that served as a dentin analog. As in the finite element analysis, the crowns were 1.0-mm thick at the central fossa and 0.5-mm thick on the marginal edge. Subsequently, the crowns were divided into two groups: As-sintered (n=15) and KAPA (n=15).

The cementation process was performed in a climate room with a relative humidity of 46% and an approximate temperature of 23 °C. The process involved three cements: a zinc phosphate (as in Study III), glass-ionomer (Ketac Cem, liquid lot 638847, powder lot 642267, 3M ESPE, USA), and a 10-MDP-based cement (as in Study II). Five crowns per cement (n=5) in each group (As-sintered and KAPA) were cemented onto G10 dentin analogs using finger pressure and a following static load of 50N for 5 minutes. For the 10-MDP-based cement and initial light-curing for 2–3 seconds was done in order to facilitate the removal of excess cement. Next, each surface (mesial, distal, buccal, lingual, and occlusal) was light-cured for 20 seconds (TransLux Wave, Kulzer, Germany). The specimens were stored in deionized water for one year at 37 °C. The water was not changed during the whole year of ageing.

A universal testing machine (ZMART.PRO, Zwick/Roell, Germany) was used to evaluate the fracture strength. The specimens were placed in a water container with constant water circulation at 37 °C. A stainless steel piston (10 mm ⌀, spherical end) was advanced perpendicularly towards the occlusal surface at a rate of 1mm/min. A 3.0-mm thick ethylene propylene diene sheet (Shore hardness 90) was placed between the piston and the specimen to prevent Hertzian/cone fracture on the occlusal surface.

Fracture toughness and hardness (Study IV)

The three types of zirconia were used. Five plates (3mm x 3mm x 1mm) per type were prepared according to the ISO 14705:2016 (thickness > 0.5 mm). The plates were embedded in epoxy resin and polished as in Study III (the last polishing step was done using a cloth and a polishing suspension).
The Vickers indentations were made with the indenter DuraScan 70 G5 (Emco-test, Austria). The hardness was calculated by the software ecos Workflow Pro (Emco-test, Austria). The indentation force of 5 kgf produced consistent hardness values and well-defined cracks. Two other indentation forces were also explored (1 kgf and 10 kgf) but were discarded due to inconsistent hardness values or complete fracture of the specimens. The type of fracture, median or Palmqvist, was determined by a) polishing and inspection (130) and b) measuring the proportion between the crack length (c or l) and the half diagonal length (a) (131,132). The cracks were found to be median. The elastic modulus was taken from the literature (47). Two equations were used:

Anstis et al.'s for median cracks (131)

$$Kic = 0.016 \bullet (E/HV)^{2/5} \bullet (F/c^{3/2})$$

where Kic = fracture toughness, E is the elastic modulus (GPa), HV the Vickers hardness (GPa), F the indentation force (N), and c the radial crack length (m).

Niihara et al.'s for median cracks (132)

$$Kic = 0.129 \bullet E^{2/5} \bullet HV^{3/5} \bullet Ø^{-3/5} \bullet a^{2} \bullet c^{-3/2}$$

where Kic = fracture toughness, E is the elastic modulus (GPa), HV the Vickers hardness (GPa), $Ø$ the constrain factor ($\simeq$ 3), a the half diagonal of the indentation (μm), and c is the radial crack length (μm).

The software ImageJ version 2.0-rc-43 (Open source image processing software, Creative commons license) was used to measure the indentations and the cracks from the images produced from the ecos Workflow Pro software (Emco-test, Austria). In addition, complementary scanning electron microscope (SEM) images were also taken (LEO Ultra 55, Carl Zeiss, Germany). The specimens were prepared for SEM as has been previously described.

3.1.2 Chemical Analyses

Raman and Fourier-transform infrared spectroscopies (Study II)

Presintered and isostatically pressed CAD/CAM blocks of the three zirconias were ground into fine powders. The powders were mixed with a 10-MDP-based cement (Panavia F 2.0 cement Lot: 000055, Kuraray, Japan) using a powder-cement weight ratio of 1:2 (108). The mixtures were formed into coins (3.0 mm ⌀ x 1.0 mm) using a PMMA form (White Peaks, Germany), and the cement excess was removed using a polytetrafluoroethylene (PTFE or Teflon) spatula. A "coin" containing only the 10-MDP-based cement served as a control. The light curing of the specimens was done for 20 seconds on each side (OptiLux VCL 500, Kerr, USA), following manufacturer's recommendations. The Raman microscope (alpha300 R, WITec, Germany) used a Nd:YAG laser (532 nm wavelength), an optical objective of 100X, and an integration time of 10 seconds. The Fourier-transform infrared microscope (Hyperion3000, Bruker, Germany) used an attenuated total reflectance germanium objective in reflection mode. Both microscopes had an approximate depth of analysis of 5–10 μm. The data from each specimen (.txt or .xls) were paired in Microsoft Excel for Mac version 16.13 (Microsoft, USA). The specimens were analyzed after 48h of storage in deionized water at 37 °C or after 10,000 thermocycles (5 °C–55 °C) (Huber, VWR, USA).

X-ray photoelectron spectroscopy (Study II)

The same specimen preparation was followed as described for FTIR and RS. Additionally, fully sintered zirconias were used as control materials, and the 10-MDP-based cement was also used as a control. The analyses were conducted using the PHI 5000 VersaProbe III Scanning XPS Microprobe (Physical Electronics, USA) equipped with a monochromatic Al Kα ($h\upsilon$ = 1486.6 eV) X-ray source. The ISO 15472 (133) was used to calibrate the registered binding energy. Two peaks were used – the main peaks of gold ($Au4f_{7/2}$, at 83.96 eV) and copper ($Cu2p_{3/2}$, at 932.62 eV). Dual charge compensation was activated. Initial survey scans (0 to 1200 eV, step size 1.00 eV) were run. Next, narrow scans on the identified elements were conducted (step size 0.10 eV). The X-ray beam size was approximately 50 μm. Ion-etching was performed (argon, 81 Å/min) to remove surface contamination. The spectra were compared before and after etching.

Back scattered electron microscopy and EDX (Study II)

In Study II, in conjunction to SEM imagining, an energy selective backscattered detector (ESB) was used to get compositional information from the mixtures (LEO Ultra 55, Carl Zeiss, Germany). The elements with higher atomic numbers appeared brighter and elements with lower atomic numbers appeared darker. Prior to ESB, the mixtures were polished using SiC papers (Struers, Denmark) under constant water (#500, #1000, #2000, and #2400). Additionally, EDX analyses were performed on sites of interest – i.e., zirconia particle-agglomerations and filler particles of the 10-MDP-based cement.

X-ray diffraction (Study III)

From each group (KAPA 15 sec, KAPA 30 sec and polished), three plates (10 mm x 10 mm x 1.5/1.0 mm) of each zirconia type underwent X-ray diffraction (XRD). The diffractometer (SmartLab, Rigaku, Japan) used a Cu Kα radiation as the X-ray source at 45 kV of voltage with a current of 200 mA. The scan speed of 10°/min was complemented with a step size of 0.02°. The software TOPAS 5 (Coelho Software, Australia) (134) was used to implement the Rietveld analysis (135) to obtain the phase content of the specimens. The models of each phase were acquired from the inorganic crystal structure database (ICSD) (https://icsd.fiz-karlsruhe.de/search/basic.xhtml) (10–13) (cubic (c), tetragonal (t), rhombohedral (r), and monoclinic (m), respectively). The atomic positions and the thermal parameters were fixed during the Rietveld refinement. The cubic phase required texture correction using spherical harmonics. The Rietveld refinement was accompanied by the estimation of the monoclinic volume fraction (Vm) using the Garvie and Nicholson method (136) modified by Toraya (137):

$$Vm = 1.311 \times Xm / (1 + 0.311 \times Xm)$$
$$Xm = [Im(-111) + Im(111)] / [Im(-111) + Im(111) + It(101)]$$

where It is the integrated intensity of the tetragonal phase and Im is the integrated intensity of the monoclinic phase. The integrated intensities of both phases were estimated by the software PDXL (Rigaku, Japan). The monoclinic phase volume fraction was expressed as the percentage of the tetragonal phase.

3.1.3 Surface morphology analysis

Interferometry (Study III and Study IV)

Three specimens from each group were analyzed using a white-light interferometer (SmartWLI extended, Gbs, Germany) at three randomly selected points (Figure 12).

Figure 12. Illustration of the specimens analyzed using interferometry.

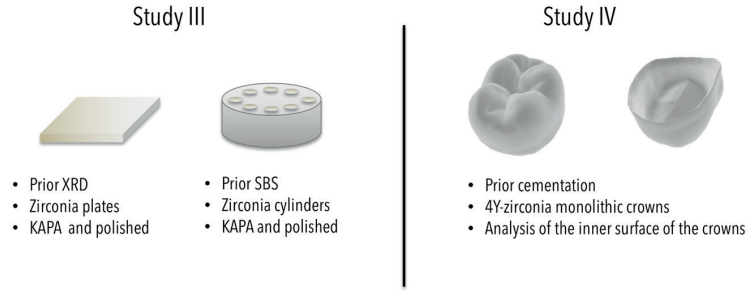

The interferometer used a 50X Mirau objective with a height resolution of 0.1 nm. An anti-vibration supporting device (Nanoseries, Accurion, Germany) situated under the interferometer was activated during the measurements. SmartVIS3D software version 2.1 (Gbs, Germany) was used to acquire surface data. The scanned area was 350×220 μm. Subsequently, the data were processed by the software MountainMaps version 7.4 (Digital Surf, France). The processing of the data consisted of a high-pass Gaussian filter (50x50 μm) as suggested by Wennerberg and Albrektsson (138). The following variables were of interest: (a) Sa (μm) – i.e., average roughness; (b) Sdr (%) – i.e., additional surface area contributed by the roughness; and (c) Sds ($1/\mu m^2$) – i.e., density of summits. Additionally, in Study IV the variable Ssk (unitless) was studied as it describes the valley or peak predominance of a surface. The surface profile of Study III was analyzed using the software ImageJ version 2.0-rc-43 (Open source image processing software, Creative commons license).

3.1.4 Statistical methods

All statistical analyses were performed with the SPSS software package, version 24 (IBM, USA). A type I error of less than 5% ($p<0.05$) was chosen as statistical significance. All the variables were analyzed to assess the distribution of the data (parametric/non-parametric). The Shapiro-Wilk test was recommended by the software manufacturer according to the sample size in each study. After the data showed to be normally distributed (parametric), groups were compared using one-way ANOVA test. The traditional zirconia (3Y-zirconia) was used as control material in post-hoc tests in Studies II, III, and IV (Dunnett test). A Tukey HSD test was conducted in Study III regarding the interferometry data. Paired t-tests were also performed to compare the same type of zirconia, but with different surface treatment, cement material, or ageing method in Studies II, III, and IV.

In Study I, three general linear models (GLM) were produced (one each for crown, cement, and dentin). The GLMs contained the interaction of four variables in the resultant von Mises stress. The variables were number of loading points, magnitude of the force, direction of the force, and elastic modulus of the cement. Eta-squared (η^2) was used to estimate the effect size of each variable in the model. The effect size of each variable was classified as small when $0.02 \leq \eta^2 < 0.13$, medium when $0.13 \leq \eta^2 < 0.26$, and large when $0.26 \leq \eta^2$.

4 RESULTS

4.1.1 Mechanical Analyses

Finite element analysis (Study I)

As can be observed in Figure 13, none of the materials reached its proportional limit. Loading condition 8 denoted the most stress for the crown and dentin – one loading point (600N at 19.5°). Loading condition 6 represented the most stress for the cements – five loading points (600N at 19.5°). The zone with the maximal stress was the marginal zone on the distal plane for the cements. None of these represented a lower or higher accumulation of stress in the crown or dentin, including the conceptual cement with mechanical properties similar to dentin.

Figure 13. Proportional limit in relation to the maximum von Mises stress reached by every material.

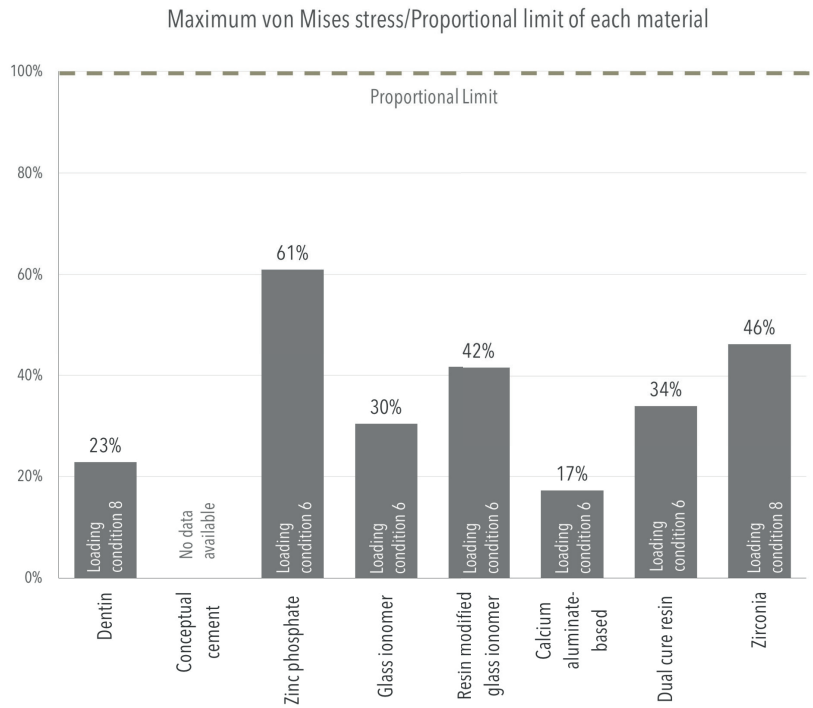

According to the GLMs, the variable "elastic modulus of the cement" had 0% effect size on the variation of the maximum von Mises stress on the crown and dentin. The GLMs could explain 88% of the variation of von Mises stress in the crown, 93% of the variation in the cements, and 94% of the variation in the dentin. The variables that had the largest effect size were number of loading points (55% of the variation) for the crown, magnitude of the force (72% of the variation) for the cement, and magnitude of the force (70% of the variation) for the dentin (Figure 14).

Figure 14. General Linear Models. Size effect of each variable.

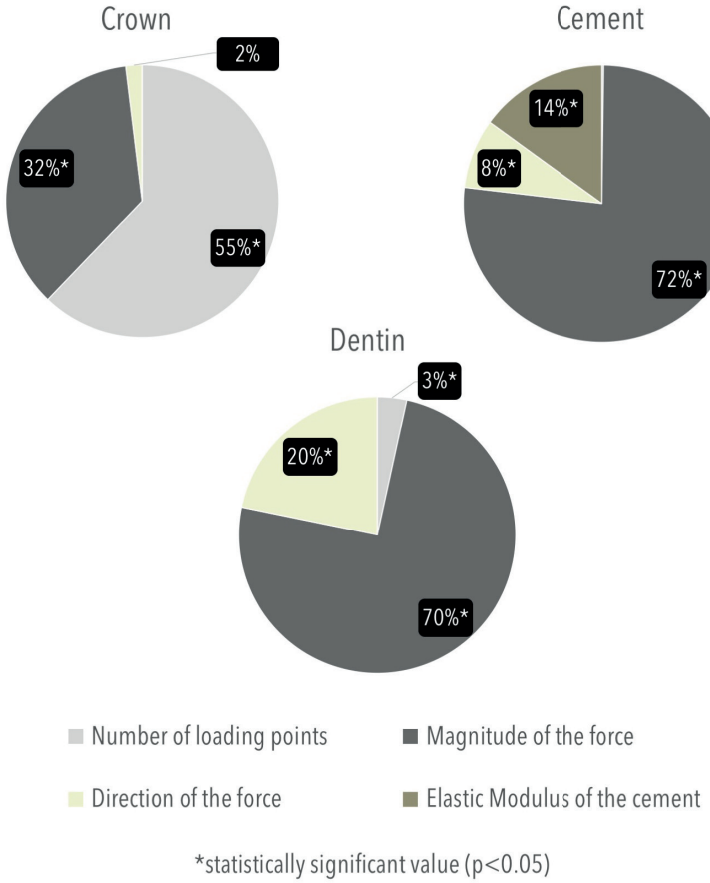

Shear bond strength (Study II and III)

Figure 15 shows the mean values with their respective standard deviations. Overall, KAPA-treated specimens combined with the 10-MDP-based cement provided the highest SBSs after 24 hours of storage at 37 °C. However, thermocycling (10,000x) reduced significantly ($p<0.05$, paired t-test) those values to approximately one-third of the initial values. The polished specimens used in combination with the 10-MDP-based cement showed to be significantly higher SBSs ($p<0.05$) than those KAPA treated in combination with zinc phosphate. No differences were observed among the types of zirconia in any group ($p>0.05$). Only 3Y- and 4Y-zirconias differed in the KAPA + zinc phosphate group ($p<0.05$).

Figure 15. Shear bond strength results. Study II and Study III.

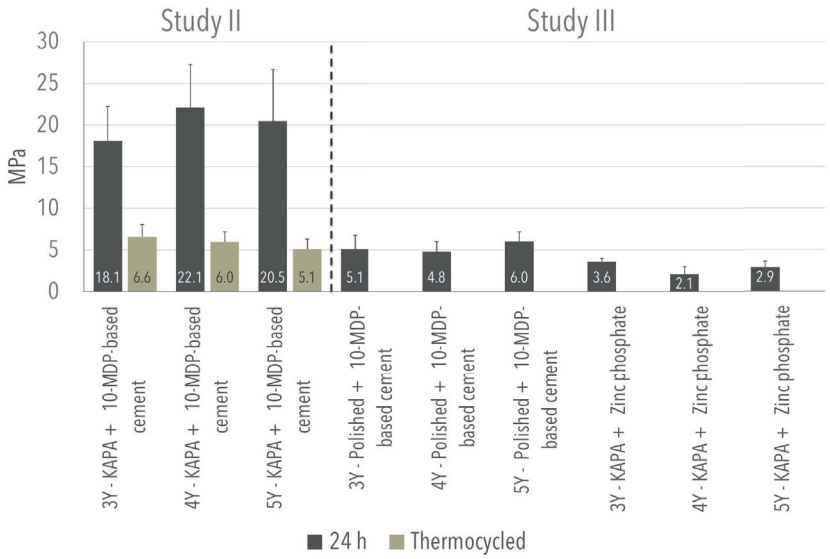

Fracture strength (Study IV)

After the ageing process (one year in deionized water at 37 °C), the registered mean fracture strengths for the monolithic 4Y-zirconia crowns were all above 4000 N (Figure 16). No statistically significant differences were observed between the two groups (As-Sintered and KAPA) and between the cements.

Figure 16. Mean fracture strengths after one year of ageing with standard deviations.

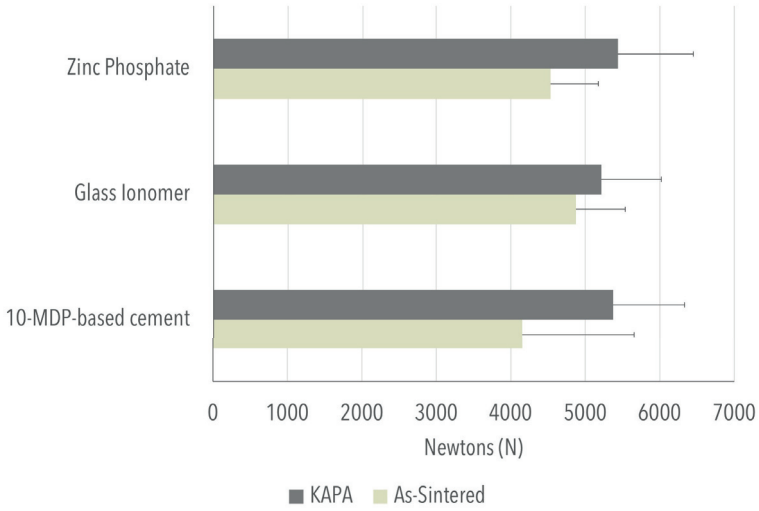

Fracture toughness and hardness (Study IV)

Regarding the hardness, statistically significant differences were found between the control (3Y-zirconia) and the other two zirconias (4Y- and 5Y-zirconias). The fracture toughness of the zirconias varied depending on the equation, and statistically significant differences were found between them.

Figure 17. Fracture toughness and hardness.

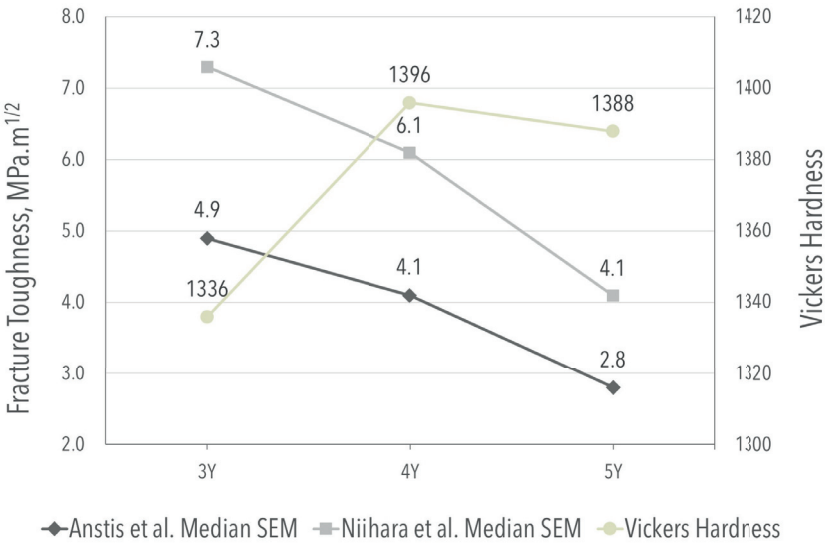

4.1.2 Chemical analyses

Raman and Fourier-transform infrared spectroscopies (Study II)

Table 6 summarizes the functional groups found by the Raman and Fourier-transform infrared spectroscopies.

Table 6. Functional groups found in the mixtures and controls.

Functional group	Type of vibration	Wavenumber, cm^{-1} (Reference)	Found in	Notes
Y-zirconia	Symmetric	120–700 (139)	All three mixtures	
Silica SiO_2	Symmetric	474 (140)	10-MDP-based cement	Mostly found in control 10-MDP-based cement
Phosphate PO_3^{2-}	Symmetric	900–1010 (30)	10-MDP-based cement & Mixtures	
Phosphate PO_3^{2-}	Asymmetric	1055–1140 (30)	10-MDP-based cement & Mixtures	Diminished in control after thermocycling
Aromatic C=C	Symmetric	1610 (142)	10-MDP-based cement & Mixtures	
Aliphatic C=C	Symmetric	1640 (142)	10-MDP-based cement & Mixtures	

X-ray photoelectron spectroscopy (Study II)

Information from the control materials provided inherent binding energies and an estimation of their composition. Scans of the three zirconias showed that zirconium (Zr) and yttrium (Y) were their main components in the Zr^{4+} and Y^{3+} states. Hafnium was registered in the scanning, but its concentration was too low (<1.0 at%) for analysis. Scanning of the filler portion of the 10-MDP-based cement showed the presence of silicon in the Si^{3+} state, aluminum in the Al^{+3} state, and barium in the Ba^{2+} state at an atomic ratio of 9:2:1. The filler particles were a combination of aluminosilicate (SiO_2/Al_2O_3) and baria given the atomic ratio. The analysis of the mixtures was based on the first electron shell of oxygen (O1s) to provide an insight into the oxide states and the suspected Zr-O-P bond (Figure 18). Binding energies that corresponded to diverse metal oxides were found. The Zr-O-P bond that has been previously registered at ≈ 531.5 eV was masked by the binding energy of silica. In the mixtures at 48 hours, the zirconia peak was dominant; however, after thermocycling, the SiO_2/Al_2O_3 + Zr-O-P peak was dominant.

Figure 18. Scans of the oxide states, first electron shell of oxygen, Os1.

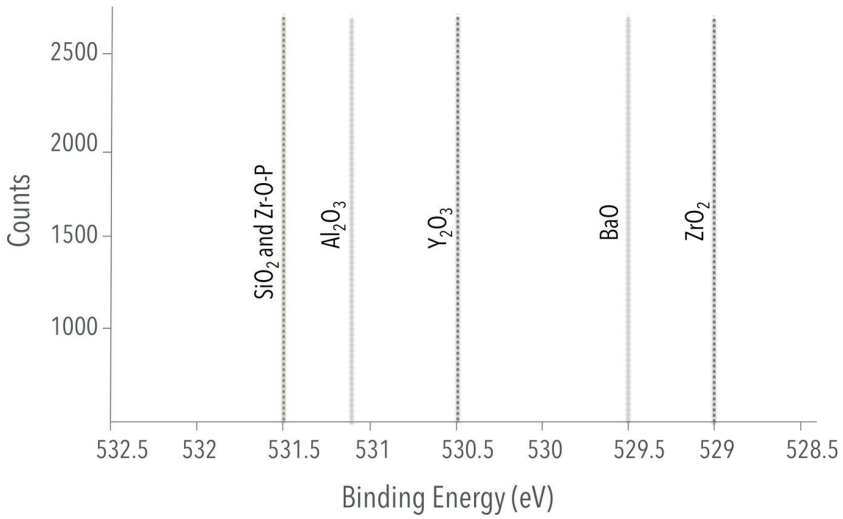

Electron backscatter microscopy and EDX (Study II)

Backscattered electron images of the thermocycled mixtures provided an insight into the atomic mass differences of the components and their delimitations (Figures 19 and 20). Lighter zones represent a higher atomic mass (zirconia and filler particles) compared to the darker areas (predominately carbon).

The EDX analyses showed that the agglomerations were constituted by oxygen (O), zirconium (Zr), and yttrium (Y). The filler particles by oxygen (O), silicon (Si), aluminum (Al), and barium (Ba).

Figure 19. Electron back scattered image of the thermocycled 4Y-zirconia + 10-MDP-based cement.

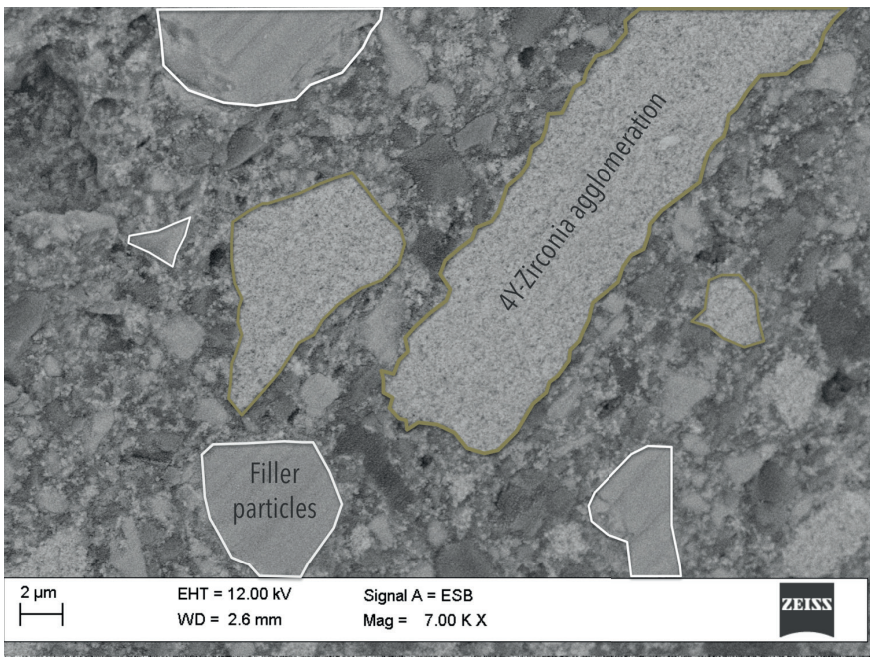

Figure 20. Electron back scattered image of the thermocycled 5Y-zirconia + 10-MDP-based cement.

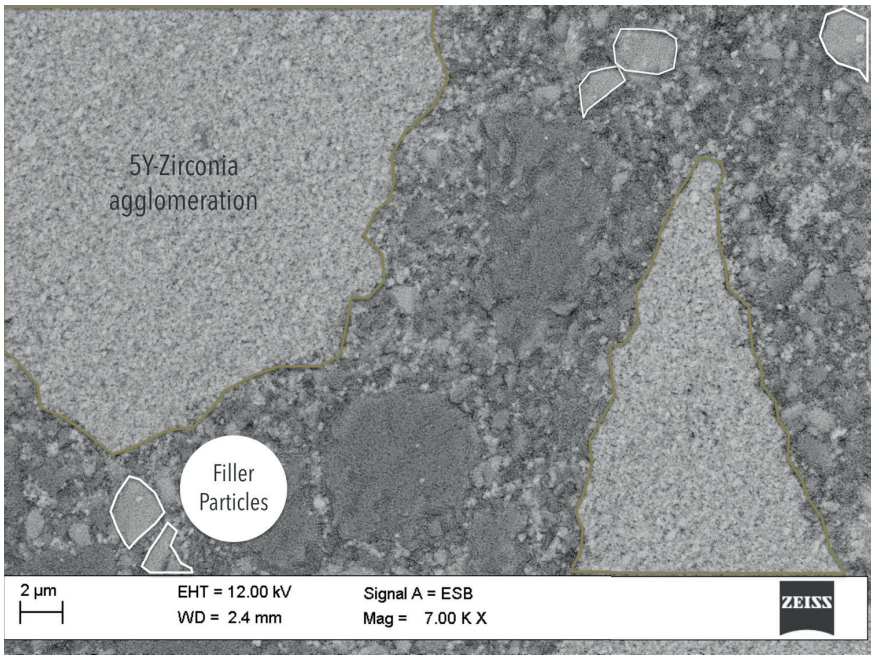

X-ray diffraction (Study III)

The results of the Rietveld refinement are illustrated in Figure 21. Results provided by the Garvie and Nicholson method modified by Toraya showed the following monoclinic percentage of the tetragonal phase (Vm%):

- 3Y-zirconia, 15 sec: 10% (±4%), 30 sec: 7% (±0.2%) and polished 0%;
- 4Y-zirconia, 15 sec: 3% (±0.1%), 30 sec: 2% (±0.3%) and polished 0%; and
- 5Y-zirconia, 15 sec: 1% (±0.5%), 30 sec: 1% (±0.3%) and polished 0%.

Figure 21. Rietveld refinement, wt%.

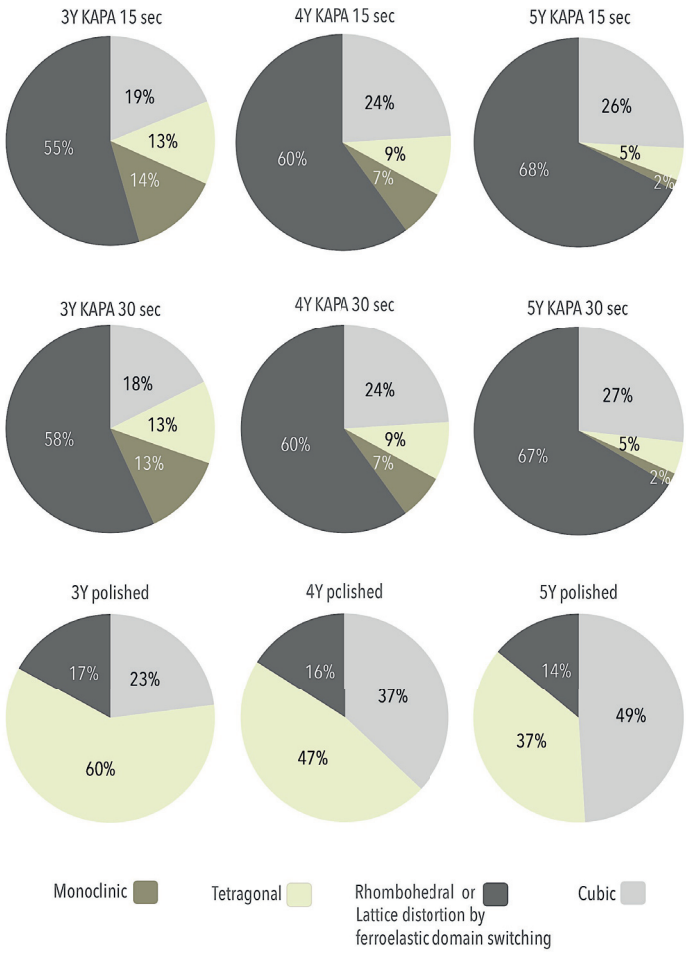

4.1.3 Surface morphology analysis

Interferometry (Study III and IV)

In Study III, regardless of the time period (15 sec or 30 sec), the three types of zirconias showed a surface roughness (Sa) in the range of 0.38–0.42 µm. No statistically significant differences (p>0.05) were found by the paired t-tests in surface developed ratios (Sdr) and density of summits (Sds) (Figure 22). However, for 4Y-zirconia, KAPA 15 sec was statistically significantly higher (p<0.05) at 15 sec.

Figure 22. Surface morphology of the treated 5Y-zirconia.

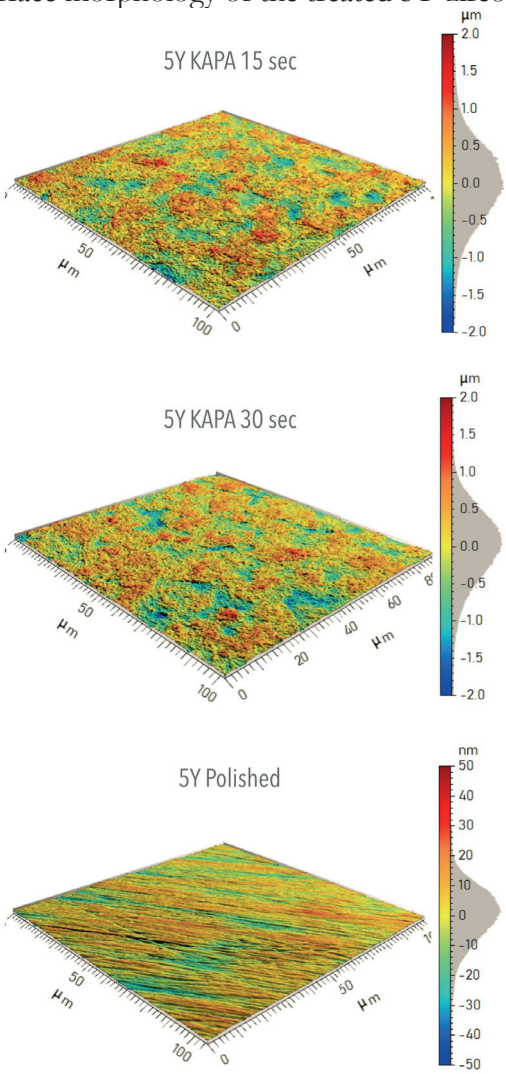

In Study IV, the as-sintered and KAPA groups showed mean surface roughness of 0.42 µm and 0.46 µm, respectively. Statistically significant differences (p<0.05) were found in the buccal and lingual surfaces. The Sdr values were around 100% for as-sintered crowns and 130% for the KAPA group. For both groups, the density of summits was approximately 1.6/µm^2. The as-sintered group showed a peak dominance (Ssk: 0.14) and the KAPA crowns a valley dominance (Ssk: -0.12) (Figure 23).

Figure 23. Intensity images of the inside of the crowns.

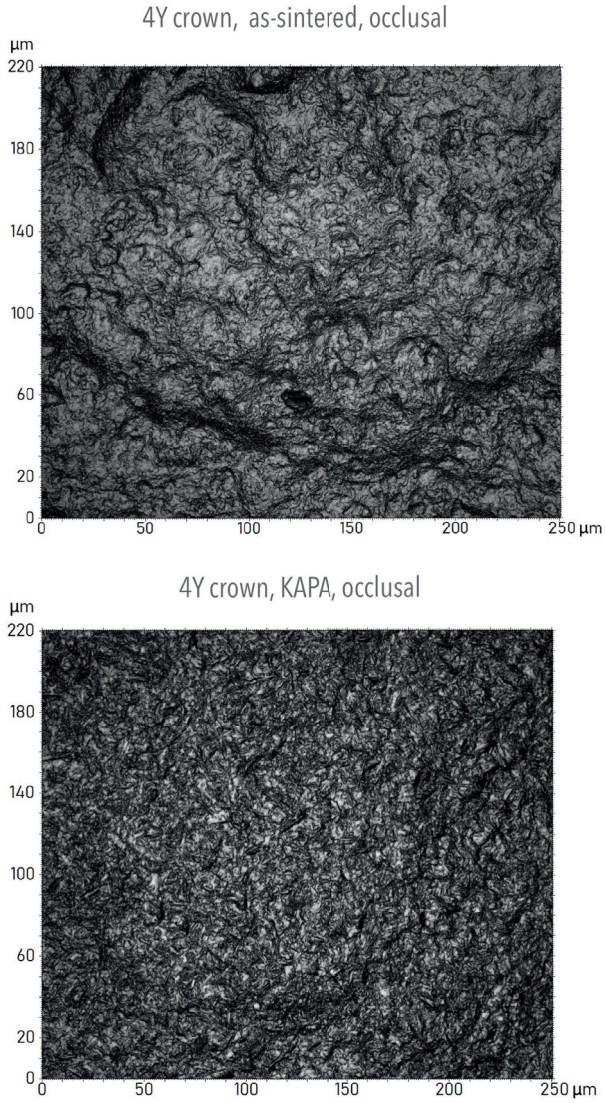

5 DISCUSSION

5.1.1 Effect of the cement

On stress distribution

According to the finite element analysis (FEA) presented in this thesis, cements with higher elastic modulus presented higher stress concentrations (theoretical cement and zinc phosphate). Similar findings have been reported by other FEAs (145–148). The marginal region was the zone with higher stress concentrations for the cements, a finding also reported in other FEA studies (127,149). Although the ideal mechanical properties of cements have been a topic of interest (77), different approaches exist. A stress-absorbing cement or "cushion" would theoretically lower the stress accumulation of the restoration by absorbing and distributing stress (148). The FEA presented in this thesis explored the "monoblock" theory or a cement with equal or similar mechanical properties of dentin serving as an extension of the remaining tooth structure. Neither the cement with the lowest elastic modulus (calcium-aluminate based), nor the "monoblock" were associated with a decrease in the stress produced on dentin or the crown. Most of the stress was concentrated on the crown. The direction of the force (19.5°) was extracted from a clinical report (121); however, due to the small sample size in that study (n=3), the direction of the force may be a limitation. The other direction (0°) denotes what has been traditionally used in other FEAs (145–147,150–152).

The influence of the periodontal ligament was omitted. The high variability reported in the literature regarding its elastic modulus and Poisson's ratio was the principal factor (153,154). However, it has been suggested that it is of importance in FEAs (155).

The FEA presented in this thesis used a non-homogeneous cement thickness, a first in dental research, that was thicker on the occlusal surface than the axial surfaces. Because this property of the cement has been observed in several descriptive clinical studies (119,156–161), it seemed appropriate to use. The mechanical properties of the materials used in the present study were obtained from diverse sources that used different experimental methods. Dentin, for example, has had an increase in the dispersion of the reported elastic

modulus values over the past 50 years, reporting a standard deviation of 4.0 GPa and a mean of 13.2 GPa. Nevertheless, recent consensus among more precise experimental methods has been able to narrow the range to 18–20 GPa for physiologic loading conditions (124).

The findings provided by the FEA of this thesis are limited because it was impossible to include clinical variables such as flaws in the crown material, voids in the cement, or modified inner surface of the crown. Collecting this information from clinical findings would be demanding. Moreover, FEAs are based on a reductionist approach to reality-based problems. That is, the objects are modeled into parts or elements that necessarily simplify their geometry; a tetrahedral form is the most common. The degrees of freedom of the model usually reflect both element size and complexity. The FEA presented in this thesis had 525,734 elements and 2'488.941 degrees of freedom. More advanced FEAs with access to resources such as high-resolution mirco-tomography and super-computer processing power have reported 100 million elements and 300 million degrees of freedom (162). Such advanced resources could provide improved possibilities to model details of the inner surface, among other advantages.

On fracture strength

The results of the FEA included in this thesis agree with the fracture strength in Study IV. No statistically significant differences were reported when comparing the fracture strength of monolithic 4Y-zirconia crowns when cemented with the three cements. Similar finding were documented by Nakamura et al. (87), who presented fracture strengths of 4000N to 5000N of monolithic 3Y-zirconia cemented with different cements. Nonetheless, the fracture strength study presented in this thesis included an additional year of ageing and fracture in water at 37 °C, a dentine analog material (G10)(123,163), and the inclusion of the KAPA protocol. These experimental factors were aimed to challenge the cements and the monolithic 4Y-zirconia crowns in terms of water absorption, dimensional changes, and possibly low temperature degradation. No significant advantage was seen for the crowns cemented with the 10-MDP-based cement compared to zinc phosphate and glass-ionomer. Nonetheless, the KAPA protocol resulted in an increased mean value in fracture strength irrespective of the cement. However, another clinically relevant design could have had been to use an experimental

setting in which the crowns de-cemented after cyclic loading. Fracture is uncommon for veneered 3Y-zirconia crowns, accounting for 0.4% of complications over five years (164). On the other hand, de-cementation or loss of retention is estimated to be 4% for the same period (90). To date, no information exists regarding complication rate and clinical outcome of the new translucent zirconia formulations. Nevertheless, the main objective with the fracture strength study was to observe the effect of different cements and KAPA treatment on the fracture strength of monolithic 4Y-zirconia crowns. Water could negatively influence the fracture properties of some ceramic materials (83). Specifically, water present during cyclic loading could lead to fatigue of the ceramic material. The phenomenon, termed "chemically assisted crack growth" in glass-ceramics (83), may also affect zirconia ceramics. This topic will be discussed in the following sub-chapter given its closely proximity to fracture toughness.

5.1.2 Fracture toughness and chemically assisted crack growth

Fracture toughness was of special interest in this thesis given that flaws and defects are unavoidable during the manufacturing process or by the clinical service of materials. Traditional formulations (3Y-zirconia) have been largely investigated using a wide variety of experimental procedures: indentation fracture (IF)(165–170,130), single-edge pre-cracked beam (SEPB)(171), single-edge v-notched beam (SEVNB)(167,172,173) surface crack in flexion (SCF)(174), chevron notched beam (CNB)(175), and double torsion (DT)(45). Nevertheless, 4Y-zirconia have only been investigated using DT (45), and 5Y-zirconia using DT (45) and SEVNB (49).

Fracture toughness estimated by indentation fracture has shown the greatest variability among the methods used. More than 10 equations exist for the estimation of fracture toughness (176), and different criteria exist for the determination of the fracture type, for example:

a) Anstis et al. criteria (131): $c \geq 2a$ = median
$c < 2a$ = Palmqvist,

b) Niihara et al. criteria (132): $c \geq 2.5a$ = median
$0.25 \leq l/a \leq 2.5$ = Palmqvist.

where c and l: crack length, and, a: half diagonal length.

The two translucent zirconias (4Y- and 5Y-zirconia) followed Anstis et al.'s criteria for median cracks. The traditional formulation, however, had a proportion of c = 1.8a. Nonetheless, the polishing and inspection method revealed median cracks in all types of zirconia. Further research is needed to standardize the criteria and determination method for this type of fracture toughness estimation. The ISO 6872:2015 recommends other methods to determine the fracture toughness of zirconia – specifically, the SEPB, CNB, and SCF methods. Moreover, the same standard does not recommend other methods such as IF and SEVNB. The first due to undisclosed reasons, but possibly because of the wide variation among equations and published results, as previously mentioned. And the latter due to the "difficulties in forming a sharp notch-tip radius" resulting in over-estimations in the fracture toughness of zirconia.

The same standard (6872:2015) has a series of clinical recommendations based on fracture toughness, resulting in five classes of dental ceramics (Table 7). These recommendations are based on clinical information (4). Nevertheless, it is not disclosed in the standard which clinical studies were included, how adhesive cementation can be recommended for some types of ceramics and not for others, and how the recommendation on the number units was made. The following two recommendations are related to the scope of this thesis. First, adhesive cementation is recommended for ceramics with a fracture toughness of 1.0 $MPa.m^{-1/2}$ or lower. Second, single-unit restorations, including in the molar region, are recommended to have a minimum fracture toughness of 2.0 $MPa.m^{-1/2}$ and can be cemented adhesively and non-adhesively.

The fracture mechanics of ceramics is a complex field. For example, it has been reported that crack velocity (m/s) is directly proportional to the energy needed to cause fracture. In theory, the energy needed would correspond to the fracture toughness of the material itself; however, slow crack growth (SCG) has been observed at energy levels under the fracture toughness, especially under cyclic loading. In other words, fracture can occur under the fracture toughness values (177). This phenomenon, in turn, appears to be more marked in the presence of water and has been termed chemically assisted crack growth (CACG) (83). This phenomenon seems to affect both glass ceramics and polycrystalline ceramics (179).

Table 7. Clinical recommendations, ISO 6872:2015.

Class	Recommended clinical indication	Minimum Fracture toughness ($MPa.m^{-1/2}$)	Example (s) (4,45)
1	a) Monolithic ceramic for single-unit anterior prostheses, veneers, inlays, or onlays adhesively cemented. b) Ceramic for coverage of a metal framework or a ceramic substructure.	0.7	Feldspathic porcelains
2	a) Monolithic ceramic for single-unit anterior or posterior prostheses adhesively cemented. b) Fully covered substructure ceramic for single-unit anterior or posterior prostheses adhesively cemented.	1.0	Leucite reinforced Feldspathic porcelains
3	a) Monolithic-ceramic for single-unit anterior or posterior prostheses and for three-unit prostheses not involving molar restoration, adhesively, or non-adhesively cemented. b) Fully covered substructure for single-unit anterior or posterior prostheses and for three-unit prostheses not involving molar restoration, adhesively, or non-adhesively cemented.	2.0	Lithium disilicate 5Y-zirconia
4	a) Monolithic-ceramic for three-unit prostheses involving molar restoration. b) Fully covered substructure for three-unit prostheses involving molar restoration.	3.5	Alumina 4Y-zirconia
5	Monolithic-ceramic for prostheses involving four or more units or fully covered substructure for prostheses involving four or more units.	5.0	3Y-zirconia

However, the available literature covers mostly SCG rather than CACG. In glass ceramics, a decrease in fatigue strength seems to be related to a preferential dissolution of the glass at the flaw tip when cyclic compressive loads are applied (Figure 24) (178). The dissolution of the glass depends on composition (especially sensible to the presence of Na_2O in the glass), the pH (especially if alkaline), and the temperature (more marked at temperatures around 90 °C) (179).

Figure 24. Schematic illustration of chemically assisted crack growth of glass ceramics.

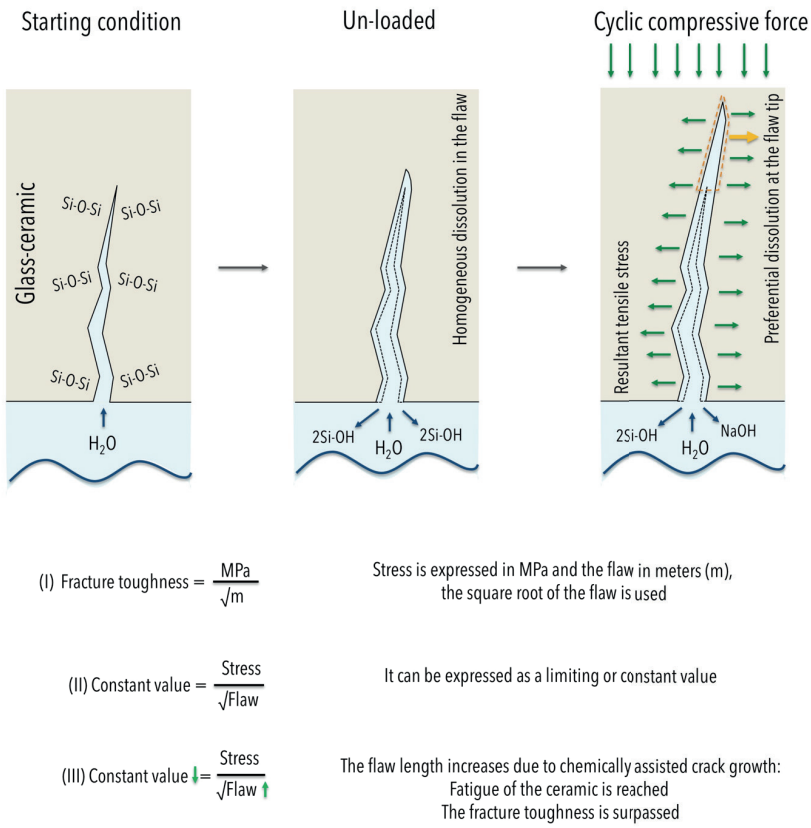

A large proportion of the research on the topic has been performed in soda lime glasses, which shares similarities with feldspathic dental porcelains, especially on the SiO_2 and Na_2O wt% (180,181). This phenomenon seems to be supported in clinical findings. The survival rate of feldspathic inlays is significantly affected when cemented with a glass-ionomer cement (water-based cement) compared to a resin-based cement (182) for 6-year period. The inlays that were cemented

with the glass-ionomer (n=59) were reported as having at least double (26.3%) the complications that led to replacement of the restoration compared to the resin-based cemented group (n=59) (12.1%) (184). Interestingly, the inlays for both groups were acid etched (4% HF), but only the resin-based cement group was silanized.

Other clinical findings show that acid etched fluoromica glass (Dicor, Dentsply, USA) single crowns cemented with zinc phosphate and glass ionomer cements had higher estimated annual risks of failure (4.5% and 3.1%, respectively) compared to a resin cement (2.0%) over 16 years (86). Both materials, feldspathic porcelain and fluoromica glass, have a fracture toughness of 0.9 $MPa.m^{-1/2}$ (183) and 1.3 $MPa.m^{-1/2}$ (184), respectively. In theory, they are susceptible to chemically assisted crack growth due to their glass content. Both would fall under ISO 6872:2015 for use with adhesive cementation limited to single units.

Another glass ceramic, lithium disilicate, has shown no statistically significant differences in single crowns when cemented with glass-ionomer or a resin cement over nine years (185). Although it has been reported that lithium disilicate is prone to SCG showing SCG at a fracture toughness of 1.0 $MPa.m^{-1/2}$, this is at least half of the reported fracture toughness of lithium disilicate (45). Nonetheless, the crowns cemented with glass-ionomer cement had a traditional retentive preparation dimension, and a thicker occlusal surface than those cemented with resin cement.

For yttria stabilized zirconia, the available literature covers traditional formulations (186–188), but is rather limited regarding translucent formulations (45). A particular study that used a traditional formulation treated the specimens with APA at a pressure of 0.25 MPa. The specimens were then subjected to one million cycles and compared to polished specimens; both groups had a thickness of 0.6 mm. The study concluded that APA reduces the fatigue strength of zirconia up to 30% and that APA should be avoided due to the possibility of creating deep microcracks and therefore other surface treatments should be considered (189). However, that study used zirconia plates and not crowns. That is, the anatomical design of a crown may have provided additional structural resistance. The specimens in that study were polished and not used as-sintered. An as-sintered surface would have been preferred as control group. The

thickness of the specimens (0.6 mm) does not seem to represent a thickness that could be used, for example, on the occlusal surface of a crown. The base material was polycarbonate, which shows an elastic modulus seven times lower than dentin (127), and probably exaggerated the tensile stresses generated at the interfaces (83). The cement material was not a commercially available cement (epoxy resin) and had an elastic modulus 2.5 lower than conventional resin cements (42) and 6 times lower than zinc phosphate (42), a condition that probably exaggerated the tensile stresses at the interfaces. The authors did not use a rubber sheet to minimize the cone/Hertzian fracture at the compressive interface (83). Finally, the test was not performed in water at 37 °C and therefore the chemically assisted crack growth could not be evaluated. However, the APA-treated specimens all had a fatigue strength over 1000 MPa.

Other investigations have shown that water could also play a significant role in chemically crack growth in zirconia, at least in the traditional formulations (186). Water seems to reduce the fracture toughness by providing, as the authors theorize, stress corrosion that resembles the dissolution of glass ceramics (188). However, an established chemical reaction has not been reported; moreover, it seems that the monoclinic content plays a significant role in increasing the fatigue strength of traditional formulations, and air-borne particle abrasion before cementation could provide the means to do this (Figure 25).

Furthermore, it has been shown in earlier studies that APA could be beneficial by increasing the flexural strength of traditional zirconia (189,190). An increase of the flexural strength by 20% compared to as-sintered specimens has been shown in water at 37 °C. The APA protocol was performed using 110-μm alumina particles at 0.4 MPa (no information about the cleaning protocol was given) (189). Other authors have reported that APA using 30-μm silica-coated alumina particles at 0.25 MPa pressure and then ultrasonically cleaned in ethanol for 10 minutes increases the fatigue limit of traditional formulations from 15% to 31% (depending on the manufacturer) measured in water at room temperature. Nonetheless, the water temperature was not set to 37 °C, no base or dentin analog was used, no commercially available cement was used, the specimens were also beveled on the edges, and the APA procedure was carried out only in the center of the specimens.

The translucent formulations seem to be prone to SCG (45); however, it is difficult to interpret results that are performed in air and not in water at 37 °C, which has been an important factor for traditional formulations in which slow crack growth could start at a fracture toughness of 3.2 MPa.m$^{-1/2}$ in water at 25 °C. That is, slow crack formation starts at 60% of the fracture toughness of traditional formulations according to previous results (45,188). There is also a need for improved knowledge regarding how much water water-based cements can transport from the oral environment into the inner surface of ceramics. Moreover, there is a need to determine whether water exposure can be prevented if amphipathic molecules, such as 10-MDP, are bonded to the surface of the ceramics.

Figure 25. Schematic illustration of chemically assisted crack growth in zirconia.

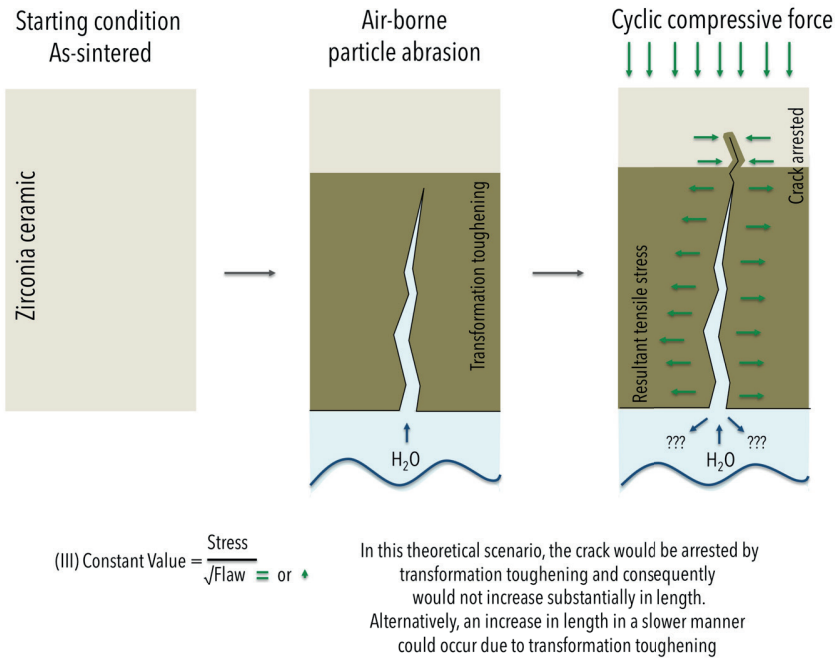

5.1.3 Effect of air-borne particle abrasion (KAPA)

On shear bond strength

In Study II, the shear bond strengths (SBS) of the 10-MDP-based cement to the APA-treated 4Y- and 5Y-zirconias were in the upper range of what has been reported in the literature for traditional formulations (10–20 MPa) (106,107,110,111,143,191). However, these studies had very different experimental settings. For example, there was no uniformity across these studies regarding the pressure of air particle abrasion, the particle size of Al_2O_3, the time of air particle abrasion, the cross-head shape, the loading rate, the surface preparation prior testing, and the ageing method. One study used storage in deionized water for 24 hours at 37 °C and a notched-edge cross-head and found similar shear bond strengths to the ones presented in this thesis (≈20 MPa) (111). A decrease in the shear bond strength has also been documented in studies that used thermocycling as an ageing method (108,191). The use of a 10-MDP-based primer could have provided additional resistance to thermocycling. On the other hand, the SBS of the 10-MDP-based cement to the highly polished and virtually flat surfaces was 5 MPa, suggesting that the KAPA protocol increases bond strength. The SBS of zinc phosphate to the zirconia that underwent KAPA treatment was approximately 3 MPa. Another study that registered the bond strength of two water-based cements to APA-treated zirconia registered SBS of 1.4 MPa (191). The mentioned study, however, used glass-ionomers, double Al_2O_3 particle size (110 μm), double pressure (0.25 MPa), and a wire loop instead of a notched edge (191). Cross-head geometry could be a major influence on stress distribution on the adhesive interface (192), at least for dentin. A notched edge or a metallic band seem to distribute the stress across the bonded specimen better than, for example, a knife or a wire loop (192,193). It is not understood how this principle could be extrapolated to ceramics and especially shear bond strength to ceramics. An ISO standard regulating these matters would be helpful.

It has been speculated that a minimum bond strength of 20 MPa could represent "clinical success". The idea can be traced back to the early 1990s, when the value of 20 MPa was based on the shear bond strength of an hydroxyethyl methacrylate (HEMA) and maleic acid adhesive to enamel (194). In principle, the idea of using value of

enamel bonding as a standard could be appropriate. However, bonding to enamel also includes the possibility of presenting secondary caries and de-bonding, which are regarded as failures. Yet, these complications could be related to an inappropriate bonding technique and not to the bond per se. Glass-ionomer, a material reporting shear bond strengths of 2–10 MPa to dentin (195), have shown to have lower annual failure rates compared to composites for class V restorations over 10 years (196). It seems that the adhesives that presented the higher shear bond strengths in vitro were correlated (R= 0.81) to lower annual failure rates for the same period. In other words, a correlation between in vitro bond strength and clinical outcome, at least in regard to dentinal bonding, has been shown. Moreover, consensus is needed to investigate whether a minimum value based on bonding to enamel can be used for ceramic materials.

On surface morphology

The surface roughness (Sa) values of the zirconia plates (Study III) were consistent among the different types of zirconias (0.4 μm, for 15 and 30 seconds). Other authors have documented values of 0.2 to 0.5 μm using pressures of 0.2–0.28 MPa in combination with 50-μm alumina particles for 15 seconds (18,197). However, the authors used different methods for obtaining the Sa – specifically, confocal laser scanning profilometer (18) and contact stylus profilometer (185). The present thesis has provided morphological results (Study III) gathered from white light interferometry. Light interferometry has better horizontal and vertical resolutions than the other two methods (138). Nonetheless, all three methods are adequate for polished and air-particle-abraded surfaces (138). Surface developed ratios (Sdrs) ranged between 116% and 134%. That is, compared to a virtually flat surface of X mm^2 through APA, another 1.2X mm^2 are created. However, the sintered surfaces of the inner surface of the crowns showed mean Sdr of 107% and consequently was not flat. That is, the milling process and subsequent sintering produced a naturally textured surface. Furthermore, quite unexpectedly, no significant differences in Sa were observed in the as-sintered group compared to the APA-treated groups. Future studies aiming to correlate Sa and SBS could provide means of optimizing the pressure of APA to provide the highest SBSs.

On phase content

The crystallographic analysis (Study III) using XRD showed the presence of monoclinic, tetragonal, rhombohedral, and cubic phases in all three types of zirconia after treated with KAPA, including the extended period of 30 seconds. Other studies reporting the effect of APA on 5Y-zirconia and 3Y-zirconia have documented the presence on the monoclinic phase content up to 2 wt% for 5Y-zirconia (18) and up to 10 Vm% for 3Y-zirconia (198). The mentioned studies used the same alumina particle size but double the pressure (0.1 MPa in Study III), and the treatment time was not documented (this thesis used an additional treatment time of 30 seconds). Other authors who have used 110-μm alumina particle size and 0.2 MPa pressure reported 15 wt% monoclinic content (199).

As previously mentioned, the rhombohedral phase is scarcely reported in dental research (18–20); other fields, however, have observed a rhombohedral phase in 2.5Y-, 3Y-, 4Y-, 5Y-, 7Y-, and 10Y-zirconias (14–17). This phase is related to the broadening of the peak at $2\theta=30°$ at the points 29.5° and 29.7° (13) and has been termed as a "hump" given its asymmetric nature (22). In this thesis, the zirconias that underwent APA according to Kern's protocol showed a high rhombohedral content (>50% wt%). It could be speculated that the low pressure (0.1MPa) was high enough to remove some material from superficial layers but also low enough to deform some cubic or tetragonal units. Moreover, the texture correction used in the Rietveld refinement (TOPAS 5, Coelho Software, Australia) could have contributed to this matter. As mentioned, the highly polished specimens showed no monoclinic content for 3Y- and 5Y-zirconias (200–202). Some rhombohedral content was detected in the highly polished specimens (13–17 wt%) and could also be related to deformation associated to the mechanical challenges of polishing.

The depth at which the XRD information was gathered was related to the phenomenon attenuation length (AL). It reflects how deep into the material X-ray photons can travel given an initial energy and a defined grazing angle (203) (Figure 26). It is also a probability; in other words, there may be X-ray photons that travel through the entire material, but the probability of this is low. If the energy of the photons is reduced to 1/e (63%), then the depth is determined as attenuation length (204).

Figure 26. Attenuation length during the XRD analysis.
a) Exponential curves of the minimum and maximum grazing angles.
b) Illustration of the depth at which most of the information was gathered

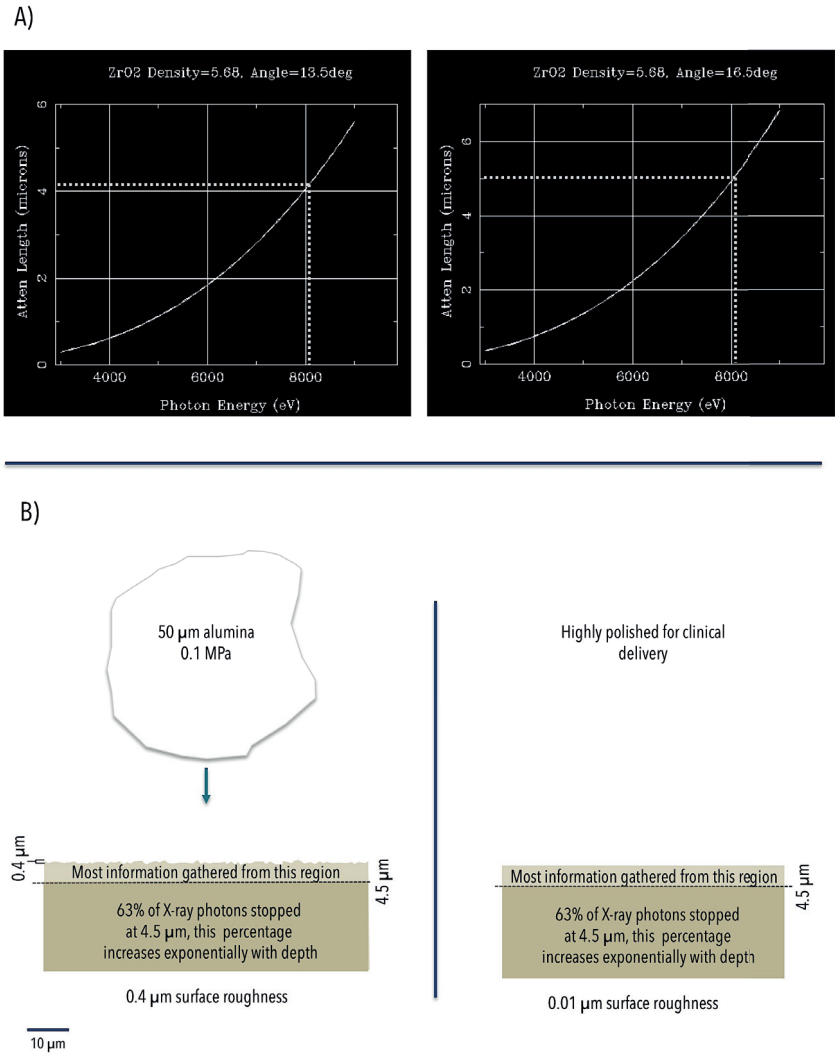

The diffractograms were produced at 2θ = 27° and 33°, which means at a grazing angle or θ of 13.5° and 16.5°. The diffractometer used Cu Kα radiation as the X-ray source, which shows an energy level of 8047 eV (204). The estimation of the AL was performed by using the service of the center for X-ray optics at the Lawrence Berkeley National Laboratory (University of California, USA). It was found that the AL was 4.1 µm to 5.0 µm and may be lower given that the density of dental zirconia is close to 6.0 gr/cm^3. This is of especial

interest given that the grain size of traditional formulations is about 0.4 μm (51) and from 0.3 to 0.8 μm for 5Y-zirconia (49). Thus, the number of "grain layers" that provided the majority of the information for the XRD analysis was between 6 and 15 layers.

5.1.4 Artificial ageing: Thermocycling and storage in water.

Ideally, in vitro tests should be based on clinical information minimizing the use of arbitrary parameters and at least resemble to some extent the clinical scenario (205). This ideal requires the pre-existence of a great amount of descriptive clinical data in order to be replicated in vitro. In this thesis, different parameters were designed to follow that philosophy, for example, the dentin analog in Study IV or the cement thickness in Study I. A controversial topic is thermocycling and water storage related to bond strength studies. To date, no study has correlated the number of thermocycles and time of clinical service. It has been postulated that 100,000 thermocycles may be needed to discriminate between adhesive systems (206). To observe changes in bond stability and mechanical degradation resembling those of the oral cavity during clinical service, a minimum of three months of water storage at 37 °C could be needed (207). Moreover, commonly used intervals for thermocycling are insufficient to provide an adequate change in temperature in the specimens, and intervals up to 60 seconds of dwell could be needed to provide appropriate temperature changes (208). The ISO standard 29022:2013, which was used as reference for Study II and Study III in this thesis, recommends water storage at 37 °C for 24 h only. Another standard – TS 11405:2016 – is also designed for measuring adhesion to tooth structure and recommends three alternatives: water storage for 24 h at 37 °C, thermocycling of 500 thermocycles (dwell time 20 seconds) after water storage for 24 h at 37 °C, and water storage at 37 °C for six months. According to the presented recommendations, the longest recommended alternative to replicate clinical findings seems to be water storage for six months at 37 °C.

5.1.5 The Zr-O-P bond

This thesis uses several analytical methods to evaluate the possible bond of 10-MDP to 4Y- and 5Y-zirconias. The FTIR analyses in Study II produced findings documented for traditional formulations (104,107,209). After thermocycling, the asymmetric vibration of the PO_3^{2-} group was diminished only in the control (10-MDP-based cement) and not in the mixtures. It is plausible that some of the molecules were dissolved in water, given that the PO_3^{2-} group is hydrophilic (101). Subsequently, these molecules had no substrate to bond to and therefore the intensity of the PO_3^{2-} peak was diminished, at least at the depth of analysis. The RS analysis found that usual peaks assigned to traditional formulations (≈ 150 cm^{-1}, 260 cm^{-1}, 330 cm^{-1}, 465 cm^{-1}, 615 cm^{-1}, and 640 cm^{-1}) (139) were also displayed by the 4Y- and 5Y-zirconias. Additionally, the mixtures showed a higher degree of polymerization after thermocycling by registering a lower intensity at the peaks 1640 cm^{-1} compared to the reference peak 1610 cm^{-1} (142). Perhaps the temperature of thermocycling (55 °C) was responsible for that phenomenon by providing additional energy to the polymer and thereby continuing the polymerization. The information provided by the XPS analyses showed that the potential Z-O-P bond was masked by the much more abundant SiO_2/Al_2O_3. The oxygen presenting ≈ 531.5 eV at the Os1 energy level is usually regarded as covalent bonding as in SiO_2/Al_2O_3. However, Nagaoka et al., using NMR, suggest that the bond is most likely ionic (110). Further research is needed to find congruence among methods to characterize the bond between Zr and 10-MDP.

The studies that used XPS as an analytical method for the investigation of the Zr-O-P bond in dental research all reported energy levels between 531.1 and 531.8 eV as reference in the Os1 analysis and as an indicator of the existence of the presumed Zr-O-P bond (106–108). All three articles refer to the same study presenting the energy level at which Zr-O-P bond could be observed with additional FTIR information as well (109). In the mentioned study, a method for producing an amorphous porous zirconium phosphate and its subsequent characterization is presented (Figure 27). Theoretically, this material is based on the Zr-O-P bond as an atomic network accompanied by some chains of 1-hydroxyethylidene. The Zr-O-P bond is identified by the authors in the range of 531.16 to 531.61 eV (113).

Figure 27. Illustration of the amorphous porous zirconium phosphate based on (113). The pores are white ellipses.

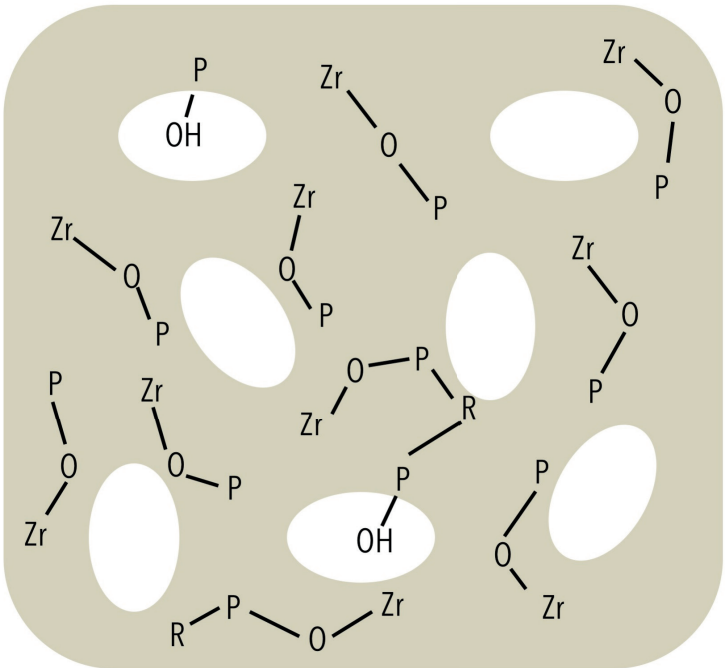

The nature of the Zr-O-P bond has been the subject of many discussions. According to the XPS information, the bond shows an energy level assigned to an oxygen that is covalently bonded (210). Moreover, when studied using NMR, the bond seems to be ionic or a hydrogen bond (110) and therefore there is a disagreement between technologies. However, few atomic bonds are purely metallic, covalent, or ionic (211).

An illustrative tool termed Van Arkel-Ketelaar triangles provides the means for calculating the extent bonds that are predominately metallic, covalent, or ionic (212) (Figure 28). The compounds are placed on the triangle by calculating the average electronegativity on the X axis and the difference in electronegativity on the Y axis (212).

Figure 28. Van Arkel-Ketelaar triangle of some binary compounds. The light purple region corresponds to semi-metallic bonds.

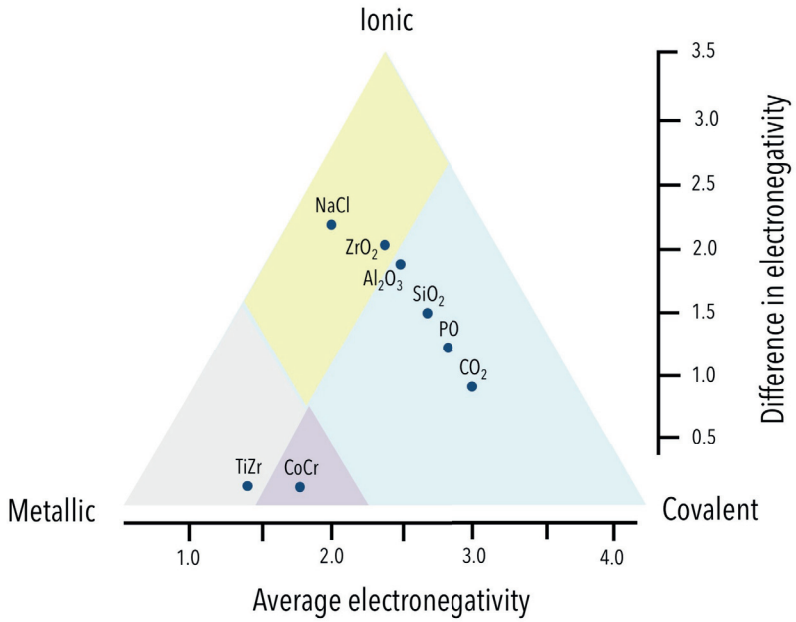

Regarding the Zr-O-P bond, two calculations are needed given that only binary compounds can be analyzed with this tool. The Zr-O bond seems to be ionic but on the proximity to the covalent region. The O-P bond appears to be on the covalent region between two compounds that are known to be covalently bonded – silica (SiO_2) and carbon dioxide (CO_2). Although bonds are rarely "pure" ionic or covalent, they may be predominately covalent and termed "polar covalent bond" when they approach the ionic region. Bonding to zirconia via 10-MDP requires further investigations to better understand the nature of the Zr-O-P, specifically its predominance.

5.1.6 The nomenclature of zirconias: The use of the adjectives "translucent", "high", "super", and "ultra"

Zirconia ceramics have been referred by different names. It is common to use 3Y-TZP (3 mol% tetragonal zirconia polycrystal) as standard for dental zirconia. Emphasis on the term tetragonal is perhaps made, given its mechanical importance in the transformation toughening process. However, in ceramic engineering, two other names appear, partially stabilized zirconia (PSZ) and fully stabilized zirconia (FSZ). The emphasis is made on the cubic content and the words "partially" or "fully" are used (23). "Fully" is commonly used for zirconias containing more than 8 mol% yttria and therefore 100% cubic (23). This variability in nomenclature could be troublesome for those who are not familiar with the terminology. In theory, a 4Y-zirconia could be categorized as 4Y-TZP given that it contains tetragonal phase, but it also could be categorized as 4Y-PSZ given that it is partially stabilized by its cubic content. The same principle applies to 3Y and 5Y formulations (Figure 29).

Figure 29. Phase diagram of 3Y-, 4Y-, and 5Y-zirconias based on (23).

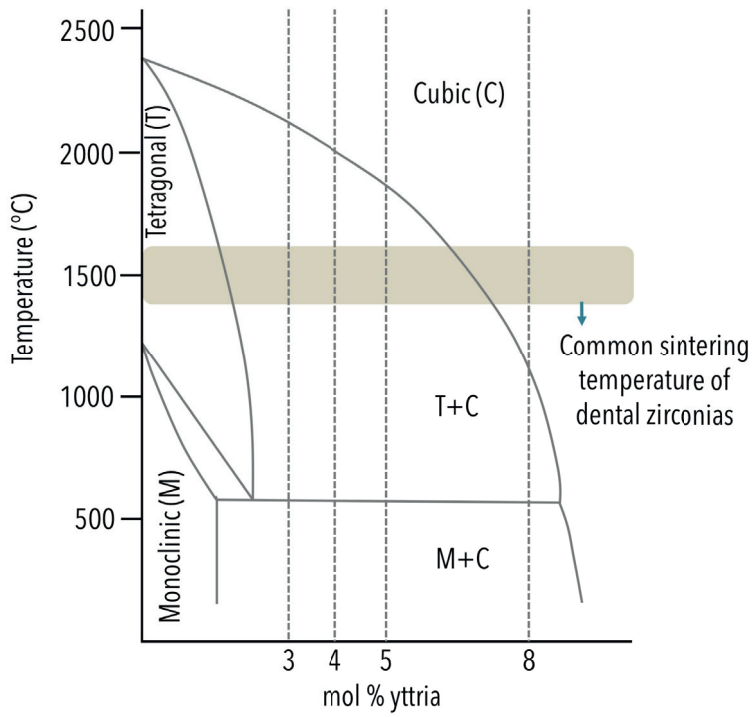

Therefore, in this thesis, these terms were simplified referring to the yttria content. This is also supported by the argument that not only the tetragonal phase is of value but also the cubic phase is of value for its contribution to the translucency.

The term "translucent" is also a matter of debate. When is a material considered translucent? How much light should the material transmit to be translucent? Is it 30%, 40%, 50%? In what thickness should the translucency be measured? Can this be regulated by some authority? If traditional formulations show a translucency of 20% (50) at 1.0-mm thickness and 5Y formulations show 24% (50) at the same thickness, is that considered a "translucent" material? Even at a reduced thickness of 0.5 mm, the increment in translucency from 3Y to 5Y is 5% (50). Therefore, the term "translucent" is mostly used as a marketing term and does not necessarily reflect a significant improvement in light transmittance.

The adjectives "high", "super", and "ultra" are also used to describe level of translucency (41,50). "High" has been used for 3Y formulations that have some form of improved translucency, for example, the 3Y formulation used in this thesis, BruxZir 2.0 HT (Glidewell, USA). "High", however, has also been used to market a 5Y formulation, Prettau Anterior (Zirkonzhan, Italy). Then there is the adjective "super", which has been used to describe a 4Y formulation, Katana ST (Kuraray Noritake, Japan) as well as to market a 5Y formulation, DDCubeX^2 (DentalDirekt, Germany). The term "ultra" has been used for a 5Y formulation, Katana UT (Kuraray Noritake, Japan). Another term has also been used, "extra", to describe a 5Y formulation, Cercon XT (Dentsply, USA). In other words, there is no agreement in how manufactures market their products and the actual yttria content of each material.

Moreover, the Merriam-Webster dictionary defines high as "situated or passing above the normal level, surface, base of measurement, or elevation", super as "exhibiting the characteristics of its type to an extreme or excessive degree", and ultra as "going beyond others or beyond due limit". Is an increment of 4% in translucency considered enough to call a material super translucent or is a 5% increment considered enough to be termed as ultra translucent?

6 CONCLUSIONS

The cement material has a negligible effect on the von Mises stress distribution of monolithic zirconia crowns. Moreover, the cement material and the KAPA protocol have no effect on the fracture strength on monolithic 4Y-zirconia crowns.

Bonding to 4Y- and 5Y-zirconias seems plausible when using a 10-MDP-based cement and implementing the KAPA protocol. However, the stability of the bond needs further research.

KAPA produces changes in the crystallographic nature of 4Y- and 5Y-zirconias. Nonetheless, the produced monoclinic phase is low and does not have any effect on the fracture strength of monolithic 4Y-zirconia crowns.

Polishing does not produce any monoclinic phase on the 4Y- and 5Y-zirconias. To perform KAPA for 15 seconds is equal to 30 seconds with respect to phase content and surface morphology.

The fracture toughness of the 4Y- and 5Y-zirconias differ compared to traditional formulations, and is inversely related to the yttria content.

7 FUTURE PERSPECTIVES

This thesis provides insight into a class of dental ceramics that have been increasing in popularity. Although they are marketed as translucent zirconias, they differ from each other at a handful of factors such as translucency, fracture toughness, yttria content, and grain size. Regulation of the use of the term "translucent" could provide clinicians a better guide when navigating the jungles of marketing. Another regulatory initiative could be the formation of an international standard regarding bonding to ceramic materials. The standard would ideally regulate factors such as the number of specimens, cross-head shape, load rate, and ageing. This approach could facilitate the comparison of results among different research groups.

Further research needs to be carried out to study the effect of the KAPA protocol on the fracture strength of monolithic 5Y-zirconia crowns and their cement alternatives. In addition, future research needs to examine low temperature degradation when using KAPA for 4Y- and 5Y-zirconias, with special emphasis on the changes to the rhombohedral phase and chemically assisted crack growth.

Finally, clinical studies of 4Y- and 5Y-zirconia based crowns are needed to provide an initial clinical understanding and potential research questions concerning the shortcomings they may present.

ACKNOWLEDGEMENTS

Victoria Franke Stenport, my main supervisor, for the relentless logistical excellence and the constant academic skepticism which improved my argumentative discourse.

Carina B. Johansson my co-supervisor, for opening the doors of academia for me, for being an extraordinary listener and supportive in difficult times. I will always be in debt with you.

Lars Hjalmarsson my co-supervisor, for always carrying a wisdom disposition, transmitting calm and patience when is most needed.

Ann Wennerberg for giving me the opportunity to learn from her by first-hand introducing me to the world of surface analysis. Not only me, but the whole research-field is always in debt with you.

Sargon Barkarmo for your friendship, for your guidance and belief in me. I look up to be half the person you are.

Keisuke Nakamura my co-author, for planting my research field so I could harvest later on, for which, I am enormously grateful. I hope you have a brilliant academic carrier.

Ketil Kvam my co-author, for your patience and opening the doors of NIOM for me, an institution always driven by excellence which I had the luck to visit and do research.

Darius Wardecki my co-author, for welcoming at your office every time it was needed and helping me navigate the world of x-ray diffraction.

Torgny Alstad for your understanding of statistics, for your friendship and constant need to leave behind a better world.

Petra H. Johansson for the company in long laboratory days, always glad to help, you are an invaluable asset to the department.

Bo Nordén for your friendship, the lunch walks, the motorcycle rides, the extremely valuable help with practical matters, for teaching

me how to press lithium-disilicate and mostly for bringing joy to the department.

Annika Uldén for opening the doors of the dental technology program for me and being always there to help with lab related problems.

Sofie Ekvall for being always helpful in ordering materials for my experiments, for being the first to believe in my pedagogical potential.

Per Svanborg for the interesting discussions which were vital to keep the research spirit up and of course the football analyses.

Johanna Petré for bringing joy to the department and making it easier to go through these years.

Veronica Graf for helping me with the ordering of materials and also being a source of liveliness in the department.

Katarina Nobelius for your help with administrative matters you are also an invaluable asset to the department.

Göran Bjerkstig for contributing in the department with honest insights and helping me with practical matters.

Peter Lundin for the invaluable advice of an experienced clinician.

Gunnar E. Carlsson for receiving me at your house, the guidance and advice in life and mostly for being a role model for me.

Malin Olsson for the company in the office during these years and the clinical advice. The future is bright for you.

Ricardo Trindade for inspiring others, including me, to love what they do by living out your passion for research.

Julia Olander, Jan Kowar, and **Rachel Duhan** my PhD colleagues I am grateful for your presence in department which helped to go through these years
Sina, Lisa and Terezia, Ema and Sofie, Malin and Karin, Oma, Annica and Shahe thanks for letting me contribute to your projects which were the source of many good research ideas.

My friends who make my life immensely more valuable, thanks for reminding me what truly matters and being there in difficult times.

Gun Johansson for your love and care, I couldn't have asked for a better welcoming period to this great country.

The Willskytt family for receiving me as one of you and being there in difficult times.

My mother Luz Angela for being an inexhaustible source of love and bravery, always ready to fight for the things you love. Te amo imensamente madre.

My father Fabio for transmitting me the constant need to feel as an individual who is responsible for its own life. Thanks for the unconditional support. Te amo enormemente padre.

My brother Santiago for occupying a great portion of my heart, always fearless to sacrifice for the better, always for growth. Te amo con todo mi corazón.

My beloved Siri all of this would have been impossible without you my love, simple as that. You are the rock on which I have constructed, you are my joy and my inspiration, my brave Siri.

Funding and assistance

This thesis was supported by Colfuturo (Fundación para el futuro de Colombia), the Sylvan Foundation, the Wilhelm and Martina Lundgren Science Foundation, the Hjalmar Svensson Research Foundation, Folktandvården Sörmland AB, the Center for Clinical Research Sörmland, Uppsala University, Eskilstuna, Sweden. The JSPS KAKENHI Grant-in-Aid for Scientific Research (C) (Grant 19K10239). Special gratitude is expressed to the departments of Chemistry and Chemical Engineering, Industrial and Materials Science and the Materials Analysis Laboratory (CMAL) of Chalmers University of Technology, Gothenburg, Sweden. And additional appreciation is given to the researchers and staff at Nordic Institute of Dental Materials (NIOM), Oslo, Norway.

REFERENCES

1. The Glossary of Prosthodontic Terms: Ninth Edition. J Prosthet Dent. 2017 May;117(5S):e1–105.

2. Montero J, Castillo-Oyagüe R, Lynch CD, Albaladejo A, Castaño A. Self-perceived changes in oral health-related quality of life after receiving different types of conventional prosthetic treatments: a cohort follow-up study. J Dent. 2013 Jun;41(6):493–503.

3. Tandvård - Antal åtgärder per år och dess medianpriser 2018. [Internet]. [cited 2020 Feb 11]. Available from: https://www.forsakringskassan.se/statistik/ovrigaersatt/tandvard

4. Kelly JR. Ceramics in Dentistry: Principles and Practice. Quintessence Publishing Company, Incorporated; 2016. 117 p.

5. Kelly JR, Benetti P. Ceramic materials in dentistry: historical evolution and current practice. Aust Dent J. 2011 Jun;56 Suppl 1:84–96.

6. Weinstein LK, Weinstein AB. Fused porcelain-to-metal teeth [Internet]. US3052982A, 1962 [cited 2020 Jan 24]. Available from: https://patents.google.com/patent/US3052982A/en

7. Boutin P. [Alumina and its use in surgery of the hip. (Experimental study)]. Presse Med. 1971 Mar 20;79(14):639–40.

8. Christel PS. Zirconia: the second generation of ceramics for total hip replacement. Bull Hosp Jt Dis Orthop Inst. 1989;49(2):170–7.

9. Garvie RC, Hannink RH, Pascoe RT. Ceramic steel? Nature. 1975 Dec;258(5537):703.

10. Yashima M, Hirose T, Katano S, Suzuki Y, Kakihana M, Yoshimura M. Structural changes of ZrO 2 - CeO 2 solid solutions around the monoclinic-tetragonal phase boundary. Physical Review B. 1995 Apr 1;51(13):8018–25.

11. Yashima M, Sasaki S, Kakihana M, Yamaguchi Y, Arashi H, Yoshimura M. Oxygen-induced structural change of the tetragonal phase around the tetragonal–cubic phase boundary in ZrO_2–$YO_{1.5}$ solid solutions. Acta Crystallographica Section B Structural Science. 1994 Dec 1;50(6):663–72.

12. Horiuchi H, Schultz AJ, Leung PCW, Williams JM. Time-of-flight neutron diffraction study of a single crystal of yttria-stabilized zirconia, Zr(Y)O1.862, at high temperature and in an applied electrical field. Acta Cryst B. 1984 Aug 1;40(4):367–72.

13. Scott HG. The yttria–zirconia δ phase. Acta Cryst B. 1977 Jan 15;33(1):281–2.

14. Kitano Y, Mori Y, Ishitani A, Masaki T. Rhombohedral Phase in Y2O3-Partially-Stabilized ZrO2. Journal of the American Ceramic Society. 1988;71(1):C-34-C–36.

15. Hasegawa H, Hioki T, Kamigaito O. Cubic-to-rhombohedral phase transformation in zirconia by ion implantation. J Mater Sci Lett. 1985 Sep 1;4(9):1092–4.

16. Roa JJ, Turon-Vinas M, Anglada M. Surface grain size and texture after annealing ground zirconia. Journal of the European Ceramic Society. 2016 May 1;36(6):1519–25.

17. Wei C, Gremillard L. The influence of stresses on ageing kinetics of 3Y- and 4Y- stabilized zirconia. Journal of the European Ceramic Society. 2018;38(2):753–60.

18. Inokoshi M, Shimizu H, Nozaki K, Takagaki T, Yoshihara K, Nagaoka N, et al. Crystallographic and morphological analysis of sandblasted highly translucent dental zirconia. Dental Materials. 2018 Mar 1;34(3):508–18.

19. Inokoshi M, Vanmeensel K, Zhang F, De Munck J, Eliades G, Minakuchi S, et al. Aging resistance of surface-treated dental zirconia. Dental Materials. 2015 Feb 1;31(2):182–94.

20. Cotič J, Jevnikar P, Kocjan A. Ageing kinetics and strength of airborne-particle abraded 3Y-TZP ceramics. Dental Materials. 2017 Jul 1;33(7):847–56.

21. Hasegawa H. Rhombohedral phase produced in abraded surfaces of partially stabilized zirconia (PSZ). J Mater Sci Lett. 1983 Mar 1;2(3):91–3.

22. Kondoh J. Origin of the hump on the left shoulder of the X-ray diffraction peaks observed in Y2O3-fully and partially stabilized ZrO2. Journal of Alloys and Compounds. 2004 Jul 28;375(1):270–82.

23. Chevalier J, Gremillard L, Virkar AV, Clarke DR. The Tetragonal-Monoclinic Transformation in Zirconia: Lessons Learned and Future Trends. Journal of the American Ceramic Society. 2009 Sep 1;92(9):1901–20.

24. Chevalier J, Gremillard L, Deville S. Low-Temperature Degradation of Zirconia and Implications for Biomedical Implants. Annual Review of Materials Research. 2007;37(1):1–32.

25. Kon M, Ishikawa K, Kuwayam N. Effects of zirconia addition on fracture toughness and bending strength of dental porcelains. Dent Mater J. 1990 Dec;9(2):181–92.

26. Winchester LJ. Bond strengths of five different ceramic brackets: an in vitro study. Eur J Orthod. 1991 Aug;13(4):293–305.

27. Meyenberg KH, Lüthy H, Schärer P. Zirconia posts: a new all-ceramic concept for nonvital abutment teeth. J Esthet Dent. 1995;7(2):73–80.

28. Luthardt RG, Sandkuhl O, Reitz B. Zirconia-TZP and alumina--advanced technologies for the manufacturing of single crowns. Eur J Prosthodont Restor Dent. 1999 Dec;7(4):113–9.

29. Cehreli MC, Kökat AM, Akça K. CAD/CAM Zirconia vs. slip-cast glass-infiltrated Alumina/Zirconia all-ceramic crowns: 2-year results of a randomized controlled clinical trial. J Appl Oral Sci. 2009 Feb;17(1):49–55.

30. Zhang Y. Making yttria-stabilized tetragonal zirconia translucent. Dental Materials. 2014 Oct 1;30(10):1195–203.

31. Yamashita I, Tsukuma K. Light scattering by residual pores in transparent zirconia ceramics. Journal of the Ceramic Society of Japan. 2011;119(1386):133–5.

32. Krell A, Klimke J, Hutzler T. Transparent compact ceramics: Inherent physical issues. Optical Materials. 2009 Jun 1;31(8):1144–50.

33. Matsui K, Yamakawa T, Uehara M, Enomoto N, Hojo J. Mechanism of alumina-enhanced sintering of fine zirconia powder: Influence of alumina concentration on the initial stage sintering. Advanced Ceramic Materials. 2008 Jun 1;91(6):1888–97.

34. Zhang H, Li Z, Kim B-N, Morita K, Yoshida H, Hiraga K, et al. Effect of Alumina Dopant on Transparency of Tetragonal Zirconia. Journal of Nanomaterials. 2012;2012:1–5.

35. Klimke J, Trunec M, Krell A. Transparent Tetragonal Yttria-Stabilized Zirconia Ceramics: Influence of Scattering Caused by Birefringence. Journal of the American Ceramic Society. 2011;94(6):1850–8.

36. French RH, Glass SJ, Ohuchi FS, Xu Y-N, Ching WY. Experimental and theoretical determination of the electronic structure and optical properties of three phases of ZrO 2. Physical Review B. 1994 Feb 15;49(8):5133–42.

37. Heffernan MJ, Aquilino SA, Diaz-Arnold AM, Haselton DR, Stanford CM, Vargas MA. Relative translucency of six all-ceramic systems. Part I: Core materials. The Journal of Prosthetic Dentistry. 2002 Jul 1;88(1):4–9.

38. Harianawala HH, Kheur MG, Apte SK, Kale BB, Sethi TS, Kheur SM. Comparative analysis of transmittance for different types of commercially available zirconia and lithium disilicate materials. J Adv Prosthodont. 2014 Dec;6(6):456–61.

39. Zhang F, Inokoshi M, Batuk M, Hadermann J, Naert I, Van Meerbeek B, et al. Strength, toughness and aging stability of highly-translucent Y-TZP ceramics for dental restorations. Dental Materials. 2016 Dec;32(12):e327–37.

40. Zhang F, Vanmeensel K, Batuk M, Hadermann J, Inokoshi M, Van Meerbeek B, et al. Highly-translucent, strong and aging-resistant 3Y-TZP ceramics for dental restoration by grain boundary segregation. Acta Biomater. 2015 Apr;16:215–22.

41. Zhang Y, Lawn BR. Novel Zirconia Materials in Dentistry. Journal of Dental Research. 2018 Feb;97(2):140–7.

42. Anusavice KJ, Shen C, Rawls HR. Phillips' Science of Dental Materials. Elsevier Health Sciences; 2014. 588 p.

43. Raigrodski AJ. Contemporary materials and technologies for all-ceramic fixed partial dentures: A review of the literature. The Journal of Prosthetic Dentistry. 2004 Dec 1;92(6):557–62.

44. Lange FF. Transformation toughening: Part 3 Experimental observations in the Zr02- Y203 system. J Mater Sci. 1982 Jan 1;17(1):240–6.

45. Zhang F, Reveron H, Spies BC, Van Meerbeek B, Chevalier J. Trade-off between fracture resistance and translucency of zirconia and lithium-disilicate glass ceramics for monolithic restorations. Acta Biomater. 2019 Jun;91:24–34.

46. Luo J, Stevens R. Porosity-dependence of elastic moduli and hardness of 3Y-TZP ceramics. Ceramics International. 1999 Apr 1;25(3):281–6.

47. Giraud S, Canel J. Young's modulus of some SOFCs materials as a function of temperature. Journal of the European Ceramic Society. 2008 Jan;28(1):77–83.

48. Lange FF. Transformation toughening: Part 1 Size effects associated with the thermodynamics of constrained transformations. Journal of Materials Science. 1982 Jan;17(1):225–34.

49. Nassary Zadeh P, Lümkemann N, Sener B, Eichberger M, Stawarczyk B. Flexural strength, fracture toughness, and translucency of cubic/tetragonal zirconia materials. J Prosthet Dent. 2018 Dec;120(6):948–54.

50. Harada K, Raigrodski AJ, Chung K-H, Flinn BD, Dogan S, Mancl LA. A comparative evaluation of the translucency of zirconias and lithium disilicate for monolithic restorations. J Prosthet Dent. 2016 Aug;116(2):257–63.

51. Nakamura K, Adolfsson E, Milleding P, Kanno T, Örtengren U. Influence of grain size and veneer firing process on the flexural strength of zirconia ceramics. European Journal of Oral Sciences. 2012;120(3):249–54.

52. Kobayashi K, Kuwajima H, Masaki T. Phase change and mechanical properties of ZrO2-Y2O3 solid electrolyte after ageing. Solid State Ionics. 1981 Aug 1;3–4:489–93.

53. Haraguchi K, Sugano N, Nishii T, Miki H, Oka K, Yoshikawa H. Phase transformation of a zirconia ceramic head after total hip arthroplasty. J Bone Joint Surg Br. 2001 Sep;83(7):996–1000.

54. Clarke I, Manaka M, Green D, Williams P, Pezzotti G, Kim Y-H, et al. CURRENT STATUS OF ZIRCONIA USED IN TOTAL HIP IMPLANTS. The Journal of Bone and Joint Surgery-american Volume. 2003;85:73–84.

55. Chevalier J, Deville S, Münch E, Jullian R, Lair F. Critical effect of cubic phase on aging in 3mol% yttria-stabilized zirconia ceramics for hip replacement prosthesis. Biomaterials. 2004 Nov;25(24):5539–45.

56. Cotič J, Jevnikar P, Kocjan A, Kosmač T. Complexity of the relationships between the sintering-temperature-dependent grain size, airborne-particle abrasion, ageing and strength of 3Y-TZP ceramics. Dental Materials. 2016 Apr 1;32(4):510–8.

57. Aurélio IL, Marchionatti AME, Montagner AF, May LG, Soares FZM. Does air particle abrasion affect the flexural strength and phase transformation of Y-TZP? A systematic review and meta-analysis. Dental Materials. 2016 Jun 1;32(6):827–45.

58. Dubruille J-H, Viguier E, Le Naour G, Dubruille M-T, Auriol M, Le Charpentier Y. Evaluation of combinations of titanium, zirconia, and alumina implants with 2 bone fillers in the dog. International Journal of Oral and Maxillofacial Implants. 1999;14(2):271–7.

59. Scarano A, Di Carlo F, Quaranta M, Piattelli A. Bone response to zirconia ceramic implants: an experimental study in rabbits. The Journal of oral implantology. 2003;29(1):8–12.

60. Sennerby L, Dasmah A, Larsson B, Iverhed M. Bone tissue responses to surface-modified zirconia implants: A histomorphometric and removal torque study in the rabbit. Clinical Implant Dentistry and Related Research. 2005;7(SUPPL. 1):S13–20.

61. Hoffmann O, Angelov N, Gallez F, Jung RE, Weber FE. The zirconia implant-bone interface: A preliminary histologic evaluation in rabbits. International Journal of Oral and Maxillofacial Implants. 2008;23(4):691–5.

62. Gahlert M, Röhling S, Wieland M, Sprecher CM, Kniha H, Milz S. Osseointegration of zirconia and titanium dental implants: a histological and histomorphometrical study in the maxilla of pigs. Clinical Oral Implants Research. 2009;20(11):1247–53.

63. Stadlinger B, Hennig M, Eckelt U, Kuhlisch E, Mai R. Comparison of zirconia and titanium implants after a short healing period. A pilot study in minipigs. International Journal of Oral and Maxillofacial Surgery. 2010 Jun 1;39(6):585–92.

64. Glauser R, Sailer I, Wohlwend A, Studer S, Schibli M, Schärer P. Experimental zirconia abutments for implant-supported single-tooth restorations in esthetically demanding regions: 4-Year results of a prospective clinical study. International Journal of Prosthodontics. 2004;17(3):285–90.

65. Zembic A, Sailer I, Jung RE, Hämmerle CHF. Randomized-controlled clinical trial of customized zirconia and titanium implant abutments for single-tooth implants in canine and posterior regions: 3-year results. Clinical Oral Implants Research. 2009;20(8):802–8.

66. Van Brakel R, Meijer GJ, Verhoeven JW, Jansen J, De Putter C, Cune MS. Soft tissue response to zirconia and titanium implant abutments: An in vivo within-subject comparison. Journal of Clinical Periodontology. 2012;39(10):995–1001.

67. Siddiqi A, Kieser JA, Silva RKD, Thomson WM, Duncan WJ. Soft and Hard Tissue Response to Zirconia versus Titanium One-Piece Implants Placed in Alveolar and Palatal Sites: A Randomized Control Trial. Clinical Implant Dentistry and Related Research. 2015;17(3):483–96.

68. Scarano A, Piattelli M, Caputi S, Favero GA, Piattelli A. Bacterial Adhesion on Commercially Pure Titanium and Zirconium Oxide Disks: An In Vivo Human Study. Journal of Periodontology. 2004;75(2):292–6.

69. Salihoğlu U, Boynueğri D, Engin D, Duman AN, Gökalp P, Baloş K. Bacterial adhesion and colonization differences between zirconium oxide and titanium alloys: An in vivo human study. International Journal of Oral and Maxillofacial Implants. 2011;26(1):101–7.

70. Brakel R van, Cune MS, Winkelhoff AJ van, Putter C de, Verhoeven JW, Reijden W van der. Early bacterial colonization and soft tissue health around zirconia and titanium abutments: an in vivo study in man. Clinical Oral Implants Research. 2011;22(6):571–7.

71. Sivaraman K, Chopra A, Narayan AI, Balakrishnan D. Is zirconia a viable alternative to titanium for oral implant? A critical review. Journal of Prosthodontic Research. 2018 Apr 1;62(2):121–33.

72. Custer LE. Mississippi Valley Association of Dental Surgeons. [Volume 34, Issue 5, May, 1892, pp. 392-395]. The Dental cosmos; a monthly record of dental science: Vol XXXIV [Vol 34] [Internet]. 1892; Available from: http://name.umdl.umich.edu/acf8385.0034.001

73. Bowen RL. Dental filling material comprising vinyl silane treated fused silica and a binder consisting of the reaction product of bis phenol and glycidyl acrylate [Internet]. US3066112 A, 1962 [cited 2018 Feb 1]. Available from: http://www.google.com/patents/US3066112

74. B K, A W. Poly(carboxylic acid)-fluoroalumino-silicate glass surgical cement [Internet]. US3814717 A, 1974 [cited 2018 Feb 1]. Available from: http://www.google.com/patents/US3814717

75. Stansbury JW. Synthetic dental compositions formed from cyclopolymerizable bis-acrylate and multi-functional oligomer and bonding method [Internet]. US5145374 A, 1992 [cited 2018 Feb 1]. Available from: http://www.google.si/patents/US5145374

76. Rosenstiel SF, Land MF, Crispin BJ. Dental luting agents: A review of the current literature. J Prosthet Dent. 1998 Sep;80(3):280–301.

77. Li ZC, White SN. Mechanical properties of dental luting cements. The Journal of Prosthetic Dentistry. 1999 May;81(5):597–609.

78. Trumpaite-Vanagiene R, Bukelskiene V, Aleksejuniene J, Puriene A, Baltriukiene D, Rutkunas V. Cytotoxicity of commonly used luting cements —An *in vitro* study. Dental Materials Journal. 2015;34(3):294–301.

79. Sahabi M, Sattari M, Baghban AA. Cytotoxicity Comparison of Harvard Zinc Phosphate Cement Versus Panavia F2 and Rely X Plus Resin Cements on Rat L929-fibroblasts. CELL JOURNAL. 2011;13(3):6.

80. Jolanki R, Kanerva L, Estlander T. Occupational allergic contact dermatitis caused by epoxy diacrylate in ultraviolet-light-cured paint, and bisphenol A in dental composite resin. Contact Dermatitis. 1995;33(2):94–9.

81. Alanko K, Kanerva L, Jolanki R, Kannas L, Estlander T. Oral mucosal diseases investigated by patch testing with a dental screening series. Contact Dermatitis. 1996;34(4):263–7.

82. Yoshida Y, Van Meerbeek B, Nakayama Y, Snauwaert J, Hellemans L, Lambrechts P, et al. Evidence of Chemical Bonding at Biomaterial-Hard Tissue Interfaces. J Dent Res. 2000 Feb 1;79(2):709–14.

83. Yoshida Y, Nagakane K, Fukuda R, Nakayama Y, Okazaki M, Shintani H, et al. Comparative Study on Adhesive Performance of Functional Monomers. J Dent Res. 2004 Jun 1;83(6):454–8.

84. Tian T, Tsoi JK-H, Matinlinna JP, Burrow MF. Aspects of bonding between resin luting cements and glass ceramic materials. Dental Materials. 2014 Jul 1;30(7):e147–62.

85. Tholey MJ, Swain MV, Thiel N. Thermal gradients and residual stresses in veneered Y-TZP frameworks. Dental Materials. 2011 Nov 1;27(11):1102–10.

86. Tholey MJ, Swain MV, Thiel N. SEM observations of porcelain Y-TZP interface. Dental Materials. 2009 Jul 1;25(7):857–62.

87. Nakamura K, Mouhat M, Nergård JM, Lægreid SJ, Kanno T, Milleding P, et al. Effect of cements on fracture resistance of monolithic zirconia crowns. Acta Biomater Odontol Scand. 2016 Jan 1;2(1):12–9.

88. Schmitt J, Wichmann M, Holst S, Reich S. Restoring severely compromised anterior teeth with zirconia crowns and feather-edged margin preparations: a 3-year follow-up of a prospective clinical trial. Int J Prosthodont. 2010 Apr;23(2):107–9.

89. Beuer F, Stimmelmayr M, Gernet W, Edelhoff D, Güh J-F, Naumann M. Prospective study of zirconia-based restorations: 3-year clinical results. Quintessence Int. 2010 Sep;41(8):631–7.

90. Vigolo P, Mutinelli S. Evaluation of Zirconium-Oxide-Based Ceramic Single-Unit Posterior Fixed Dental Prostheses (FDPs) Generated with Two CAD/CAM Systems Compared to Porcelain-Fused-to-Metal Single-Unit Posterior FDPs: A 5-Year Clinical Prospective Study. Journal of Prosthodontics. 2012 Jun 1;21(4):265–9.

91. Ortorp A, Kihl ML, Carlsson GE. A 5-year retrospective study of survival of zirconia single crowns fitted in a private clinical setting. J Dent. 2012 Jun;40(6):527–30.

92. Sagirkaya E, Arikan S, Sadik B, Kara C, Karasoy D, Cehreli M. A randomized, prospective, open-ended clinical trial of zirconia fixed partial dentures on teeth and implants: interim results. Int J Prosthodont. 2012 Jun;25(3):221–31.

93. Rinke S, Schäfer S, Lange K, Gersdorff N, Roediger M. Practice-based clinical evaluation of metal-ceramic and zirconia molar crowns: 3-year results. J Oral Rehabil. 2013 Mar;40(3):228–37.

94. Monaco C, Caldari M, Scotti R, AIOP Clinical Research Group. Clinical evaluation of 1,132 zirconia-based single crowns: a retrospective cohort study from the AIOP clinical research group. Int J Prosthodont. 2013 Oct;26(5):435–42.

95. Gherlone E, Mandelli F, Capparè P, Pantaleo G, Traini T, Ferrini F. A 3 years retrospective study of survival for zirconia-based single crowns fabricated from intraoral digital impressions. J Dent. 2014 Sep;42(9):1151–5.

96. Seydler B, Schmitter M. Clinical performance of two different CAD/CAM-fabricated ceramic crowns: 2-Year results. J Prosthet Dent. 2015 Aug;114(2):212–6.

97. Dogan S, Raigrodski AJ, Zhang H, Mancl LA. Prospective cohort clinical study assessing the 5-year survival and success of anterior maxillary zirconia-based crowns with customized zirconia copings. J Prosthet Dent. 2017 Feb;117(2):226–32.

98. Maroulakos G, Thompson GA, Kontogiorgos ED. Effect of cement type on the clinical performance and complications of zirconia and lithium disilicate tooth-supported crowns: A systematic review. Report of the Committee on Research in Fixed Prosthodontics of the American Academy of Fixed Prosthodontics. J Prosthet Dent. 2019 May;121(5):754–65.

99. Tzanakakis E-GC, Tzoutzas IG, Koidis PT. Is there a potential for durable adhesion to zirconia restorations? A systematic review. J Prosthet Dent. 2016 Jan;115(1):9–19.

100. Omura I, Yamauchi J, Nagase Y, Uemura F. Adhesive compositions [Internet]. US4537940A, 1985 [cited 2018 Aug 28]. Available from: https://patents.google.com/patent/US4537940A/en?assignee=kuraray&before=priority:19850101&after=priority:19800101

101. Suzuki M, Fujishima A, Miyazaki T, Hisamitsu H, Ando H, Nakahara M, et al. A study on adsorption structures of methacryloyloxyalkyl dihydrogen phosphates on silver substrates by infrared reflection absorption spectroscopy. J Biomed Mater Res. 1997 Nov 1;37(2):252–60.

102. Suzuki M, Yamamoto M, Fujishima A, Miyazaki T, Hisamitsu H, Kojima K, et al. Raman and IR studies on adsorption behavior of adhesive monomers in a metal primer for Au, Ag, Cu, and Cr surfaces. J Biomed Mater Res. 2002 Oct 1;62(1):37–45.

103. Sezinando A. Looking for the ideal adhesive – A review. Revista Portuguesa de Estomatologia, Medicina Dentária e Cirurgia Maxilofacial. 2014 Oct 1;55(4):194–206.

104. Pilo R, Kaitsas V, Zinelis S, Eliades G. Interaction of zirconia primers with yttria-stabilized zirconia surfaces. Dental Materials. 2016 Mar;32(3):353–62.

105. Xie H, Li Q, Zhang F, Lu Y, Tay FR, Qian M, et al. Comparison of resin bonding improvements to zirconia between one-bottle universal adhesives and tribochemical silica coating, which is better? Dental Materials. 2016 Mar;32(3):403–11.

106. Chen Y, Lu Z, Qian M, Zhang H, Chen C, Xie H, et al. Chemical affinity of 10-methacryloyloxydecyl dihydrogen phosphate to dental zirconia: Effects of molecular structure and solvents. Dental Materials [Internet]. 2017 Oct 14 [cited 2017 Nov 7]; Available from: http://www.sciencedirect.com/science/article/pii/S0109564117305298

107. Chen Y, Lu Z, Qian M, Zhang H, Xie H, Chen C. Effect of 10-Methacryloxydecyl Dihydrogen Phosphate Concentration on Chemical Coupling of Methacrylate Resin to Yttria-stabilized Zirconia. J Adhes Dent. 2017;19(4):349–55.

108. Xie H, Li Q, Zhang F, Lu Y, Tay FR, Qian M, et al. Comparison of resin bonding improvements to zirconia between one-bottle universal adhesives and tribochemical silica coating, which is better? Dental Materials. 2016 Mar;32(3):403–11.

109. Lin X-Z, Yuan Z-Y. Synthesis of amorphous porous zirconium phosphonate materials: tuneable from micropore to mesopore sizes. RSC Adv. 2014 Jul 24;4(61):32443–50.

110. Nagaoka N, Yoshihara K, Feitosa VP, Tamada Y, Irie M, Yoshida Y, et al. Chemical interaction mechanism of 10-MDP with zirconia. Scientific Reports. 2017 Mar 30;7:45563.

111. Chen L, Suh BI, Brown D, Chen X. Bonding of primed zirconia ceramics: evidence of chemical bonding and improved bond strengths. Am J Dent. 2012 Apr;25(2):103–8.

112. Kern M, Wegner SM. Bonding to zirconia ceramic: adhesion methods and their durability. Dent Mater. 1998 Jan;14(1):64–71.

113. Kern M, Passia N, Sasse M, Yazigi C. Ten-year outcome of zirconia ceramic cantilever resin-bonded fixed dental prostheses and the influence of the reasons for missing incisors. J Dent. 2017 Jul 5;

114. Abou Tara M, Eschbach S, Wolfart S, Kern M. Zirconia ceramic inlay-retained fixed dental prostheses – first clinical results with a new design. Journal of Dentistry. 2011 Mar 1;39(3):208–11.

115. Periodic_Table_and_X-ray_Energies.pdf [Internet]. [cited 2017 Nov 22]. Available from: https://www.bruker.com/fileadmin/user_upload/8-PDF-Docs/X-rayDiffraction_ElementalAnalysis/HH-XRF/Misc/Periodic_Table_and_X-ray_Energies.pdf

116. Nakamura K, Harada A, Inagaki R, Kanno T, Niwano Y, Milleding P, et al. Fracture resistance of monolithic zirconia molar crowns with reduced thickness. Acta Odontol Scand. 2015;73(8):602–8.

117. Ohm E, Silness J. The convergence angle in teeth prepared for artificial crowns. J Oral Rehabil. 1978 Oct;5(4):371–5.

118. Nordlander J, Weir D, Stoffer W, Ochi S. The taper of clinical preparations for fixed prosthodontics. J Prosthet Dent. 1988 Aug;60(2):148–51.

119. Pilo R, Cardash HS. In vivo retrospective study of cement thickness under crowns. J Prosthet Dent. 1998 Jun;79(6):621–5.

120. Contrepois M, Soenen A, Bartala M, Laviole O. Marginal adaptation of ceramic crowns: a systematic review. J Prosthet Dent. 2013 Dec;110(6):447-454.e10.

121. Morikawa A. [Investigation of occlusal force on lower first molar in function]. Kokubyo Gakkai Zasshi. 1994 Jun;61(2):250–74.

122. Hidaka O, Iwasaki M, Saito M, Morimoto T. Influence of clenching intensity on bite force balance, occlusal contact area, and average bite pressure. J Dent Res. 1999 Jul;78(7):1336–44.

123. Kelly JR. Clinically relevant approach to failure testing of all-ceramic restorations. The Journal of Prosthetic Dentistry. 1999 Jun;81(6):652–61.

124. Kinney JH, Marshall SJ, Marshall GW. The mechanical properties of human dentin: a critical review and re-evaluation of the dental literature. Crit Rev Oral Biol Med. 2003;14(1):13–29.

125. Rekow ED, Harsono M, Janal M, Thompson VP, Zhang G. Factorial analysis of variables influencing stress in all-ceramic crowns. Dent Mater. 2006 Feb;22(2):125–32.

126. Akinmade AO, Nicholson JW. Poisson's ratio of glass-polyalkenoate ("glass-ionomer") cements determined by an ultrasonic pulse method. J Mater Sci: Mater Med. 1995 Aug;6(8):483–5.

127. Bowley JF, Ichim IP, Kieser JA, Swain MV. FEA evaluation of the resistance form of a premolar crown. J Prosthodont. 2013 Jun;22(4):304–12.

128. Attar N, Tam LE, McComb D. Mechanical and physical properties of contemporary dental luting agents. J Prosthet Dent. 2003 Feb;89(2):127–34.

129. Lin C-L, Chang W-J, Lin Y-S, Chang Y-H, Lin Y-F. Evaluation of the relative contributions of multi-factors in an adhesive MOD restoration using FEA and the Taguchi method. Dent Mater. 2009 Sep;25(9):1073–81.

130. Ćorić D, Ćurković L, Majić Renjo M. Statistical Analysis of Vickers Indentation Fracture Toughness of Y-TZP Ceramics. Transactions of FAMENA. 2017 Jul 24;41(2):1–16.

131. Anstis GR, Chantikul P, Lawn BR, Marshall DB. A Critical Evaluation of Indentation Techniques for Measuring Fracture Toughness: I, Direct Crack Measurements. Journal of the American Ceramic Society. 1981 Sep;64(9):533–8.

132. Niihara K, Morena R, Hasselman DPH. Evaluation of KIc of brittle solids by the indentation method with low crack-to-indent ratios. Journal of Materials Science Letters. 1982;1(1):13–6.

133. M.P. Seah, Summary of ISO/TC 201 Standard: VII ISO 15472:2001 - surface chemical analysis - x-ray photoelectron spectrometers - calibration of energy scales, Surf. Interface Analy. 2001; 31; 721 - 723. [Internet]. [cited 2017 Dec 8]. Available from: http://serials.unibo.it/cgi-ser/start/en/spogli/df-s.tcl?prog_art=8402199&language=ENGLISH&view=articoli

134. Coelho AA. TOPAS and TOPAS-Academic: an optimization program integrating computer algebra and crystallographic objects written in C++. J Appl Cryst. 2018 Feb 1;51(1):210–8.

135. Rietveld HM. A profile refinement method for nuclear and magnetic structures. J Appl Cryst. 1969 Jun 2;2(2):65–71.

136. Garvie RC, Nicholson PS. Phase Analysis in Zirconia Systems. Journal of the American Ceramic Society. 1972 Jun 1;55(6):303–5.

137. Toraya H, Yoshimura M, Somiya S. Calibration Curve for Quantitative Analysis of the Monoclinic-Tetragonal ZrO2 System by X-Ray Diffraction. Journal of the American Ceramic Society. 1984;67(6):C-119-C–121.

138. Wennerberg A, Albrektsson T. Suggested guidelines for the topographic evaluation of implant surfaces. Int J Oral Maxillofac Implants. 2000 Jun;15(3):331–44.

139. Durand J-C, Jacquot B, Salehi H, Fages M, Margerit J, Cuisinier FJG. Confocal Raman microscopic analysis of the zirconia/feldspathic ceramic interface. Dental Materials. 2012 Jun;28(6):661–71.

140. Gillet P, Le CléAc'h AndréE, Madon M. High-temperature raman spectroscopy of SiO2 and GeO2 Polymorphs: Anharmonicity and thermodynamic properties at high-temperatures. Journal of Geophysical Research. 1990 Dec 1;95:21.

141. Thomas LC, Chittekden RA. Characteristic infrared absorption frequencies of organophosphorus compounds—VII. Phosphorns ions. Spectrochimica Acta Part A: Molecular Spectroscopy. 1970 Apr 1;26(4):781–800.

142. Inokoshi M, Pongprueksa P, De Munck J, Zhang F, Vanmeensel K, Minakuchi S, et al. Influence of Light Irradiation Through Zirconia on the Degree of Conversion of Composite Cements. J Adhes Dent. 2016;18(2):161–71.

143. Xie H, Li Q, Zhang F, Lu Y, Tay FR, Qian M, et al. Comparison of resin bonding improvements to zirconia between one-bottle universal adhesives and tribochemical silica coating, which is better? Dental Materials. 2016 Mar 1;32(3):403–11.

144. Lin X-Z, Yuan Z-Y. Synthesis of amorphous porous zirconium phosphonate materials: tuneable from micropore to mesopore sizes. RSC Adv. 2014 Jul 24;4(61):32443–50.

145. Kamposiora P, Papavasiliou G, Bayne SC, Felton DA. Predictions of cement microfracture under crowns using 3D-FEA. J Prosthodont. 2000 Dec;9(4):201–9.

146. Proos KA, Swain MV, Ironside J, Steven GP. Influence of cement on a restored crown of a first premolar using finite element analysis. Int J Prosthodont. 2003 Feb;16(1):82–90.

147. Rafferty BT, Janal MN, Zavanelli RA, Silva NRFA, Rekow ED, Thompson VP, et al. Design features of a three-dimensional molar crown and related maximum principal stress. A finite element model study. Dent Mater. 2010 Feb;26(2):156–63.

148. Liu B, Lu C, Wu Y, Zhang X, Arola D, Zhang D. The effects of adhesive type and thickness on stress distribution in molars restored with all-ceramic crowns. J Prosthodont. 2011 Jan;20(1):35–44.

149. Shahrbaf S, van Noort R, Mirzakouchaki B, Ghassemieh E, Martin N. Fracture strength of machined ceramic crowns as a function of tooth preparation design and the elastic modulus of the cement. Dent Mater. 2014 Feb;30(2):234–41.

150. Nakamura T, Imanishi A, Kashima H, Ohyama T, Ishigaki S. Stress analysis of metal-free polymer crowns using the three-dimensional finite element method. Int J Prosthodont. 2001 Oct;14(5):401–5.

151. Kobayashi K, Yorimoto T, Hikita K, Maida T. Abutment forms and restorative materials in adhesive prosthesis: a finite element analysis. Dent Mater J. 2004 Jun;23(2):75–80.

152. Lu C, Wang R, Mao S, Arola D, Zhang D. Reduction of load-bearing capacity of all-ceramic crowns due to cement aging. J Mech Behav Biomed Mater. 2013 Jan;17:56–65.

153. Ruse ND. Propagation of erroneous data for the modulus of elasticity of periodontal ligament and gutta percha in FEM/FEA papers: a story of broken links. Dent Mater. 2008 Dec;24(12):1717–9.

154. Fill TS, Carey JP, Toogood RW, Major PW. Experimentally Determined Mechanical Properties of, and Models for, the Periodontal Ligament: Critical Review of Current Literature. J Dent Biomech [Internet]. 2011 Apr 5 [cited 2016 Feb 3];2011. Available from: http://www.ncbi.nlm.nih.gov/pmc/articles/PMC3134825/

155. Rees JS. An investigation into the importance of the periodontal ligament and alveolar bone as supporting structures in finite element studies. J Oral Rehabil. 2001 May;28(5):425–32.

156. McLean JW, von Fraunhofer JA. The estimation of cement film thickness by an in vivo technique. Br Dent J. 1971 Aug 3;131(3):107–11.

157. Reich S, Wichmann M, Nkenke E, Proeschel P. Clinical fit of all-ceramic three-unit fixed partial dentures, generated with three different CAD/CAM systems. European Journal of Oral Sciences. 2005 Apr 1;113(2):174–9.

158. Quante K, Ludwig K, Kern M. Marginal and internal fit of metal-ceramic crowns fabricated with a new laser melting technology. Dental Materials. 2008 Oct;24(10):1311–5.

159. Reich S, Kappe K, Teschner H, Schmitt J. Clinical fit of four-unit zirconia posterior fixed dental prostheses. European Journal of Oral Sciences. 2008 Dec 1;116(6):579–84.

160. Reich S, Uhlen S, Gozdowski S, Lohbauer U. Measurement of cement thickness under lithium disilicate crowns using an impression material technique. Clin Oral Investig. 2011 Aug;15(4):521–6.

161. White SN, Yu Z, Tom JFMD, Sangsurasak S. In vivo marginal adaptation of cast crowns luted with different cements. The Journal of Prosthetic Dentistry. 1995 Jul;74(1):25–32.

162. Bekas C, Curioni A, Arbenz P, Flaig C, Van Lenthe GH, Müller R, et al. Extreme scalability challenges in micro-finite element simulations of human bone. Concurrency and Computation: Practice and Experience. 2010;22(16):2282–2296.

163. Kelly JR, Rungruanganunt P, Hunter B, Vailati F. Development of a clinically validated bulk failure test for ceramic crowns. The Journal of Prosthetic Dentistry. 2010 Oct;104(4):228–38.

164. Sailer I, Makarov NA, Thoma DS, Zwahlen M, Pjetursson BE. Corrigendum to "All-ceramic or metal-ceramic tooth- supported fixed dental prostheses (FDPs)? A systematic review of the survival and complication rates. Part I: Single crowns (SCs)" [Dental Materials 31 (6) (2015) 603–623]. Dental Materials. 2016 Dec;32(12):e389–90.

165. Studart AR, Filser F, Kocher P, Gauckler LJ. Fatigue of zirconia under cyclic loading in water and its implications for the design of dental bridges. Dent Mater. 2007 Jan;23(1):106–14.

166. Yilmaz H, Aydin C, Gul BE. Flexural strength and fracture toughness of dental core ceramics. J Prosthet Dent. 2007 Aug;98(2):120–8.

167. Aboushelib MN, Kleverlaan CJ, Feilzer AJ. Evaluation of a high fracture toughness composite ceramic for dental applications. J Prosthodont. 2008 Oct;17(7):538–44.

168. Mitov G, Gessner J, Lohbauer U, Woll K, Muecklich F, Pospiech P. Subcritical crack growth behavior and life data analysis of two types of dental Y-TZP ceramics. Dental Materials. 2011 Jul 1;27(7):684–91.

169. Nemli SK, Yilmaz H, Aydin C, Bal BT, Tıraş T. Effect of fatigue on fracture toughness and phase transformation of Y-TZP ceramics by X-ray diffraction and Raman spectroscopy. Journal of Biomedical Materials Research Part B: Applied Biomaterials. 2012 Feb;100B(2):416–24.

170. Harada K, Shinya A, Yokoyama D, Shinya A. Effect of loading conditions on the fracture toughness of zirconia. Journal of Prosthodontic Research. 2013 Apr 1;57(2):82–7.

171. Nose T, Fujii T. Evaluation of Fracture Toughness for Ceramic Materials by a Single-Edge-Precracked-Beam Method. Journal of the American Ceramic Society. 1988;71(5):328–33.

172. Marinis A, Aquilino SA, Lund PS, Gratton DG, Stanford CM, Diaz-Arnold AM, et al. Fracture toughness of yttria-stabilized zirconia sintered in conventional and microwave ovens. The Journal of Prosthetic Dentistry. 2013 Mar 1;109(3):165–71.

173. Cui J, Liu H, Guan K, Rao P. Load-deflection behavior of fracture toughness testing of ceramics by SEVNB method. International Journal of Applied Ceramic Technology. 2018;15(5):1310–5.

174. Quinn GD, Gettings RJ, Kubler JJ. Fracture toughness by the surface crack in flexure (SCF) method: Results of the VAMAS round robin. Ceramic Engineering and Science Proceedings. 1994;15(5):846–55.

175. Kailer A, Stephan M. On the feasibility of the Chevron Notch Beam method to measure fracture toughness of fine-grained zirconia ceramics. Dental Materials. 2016 Oct 1;32(10):1256–62.

176. Moradkhani A, Baharvandi H, Tajdari M, Latifi H, Martikainen J. Determination of fracture toughness using the area of micro-crack tracks left in brittle materials by Vickers indentation test. J Adv Ceram. 2013 Mar 1;2(1):87–102.

177. Olagnon C, Chevalier J, Pauchard V. Global description of crack propagation in ceramics. Journal of the European Ceramic Society. 2006 Jan 1;26(15):3051–9.

178. Benbahouche S, Roumili F, Zegadi R. Effect of Water on the Impact Strength of Glass Plates with Eroded Surfaces. Materials Science. 2003 Jan 1;39(1):148–52.

179. Ciccotti M. Stress-corrosion mechanisms in silicate glasses. J Phys D: Appl Phys. 2009 Oct;42(21):214006.

180. Joshi GV, Duan Y, Della Bona A, Hill TJ, St John K, Griggs JA. Contributions of stress corrosion and cyclic fatigue to subcritical crack growth in a dental glass-ceramic. Dent Mater. 2014 Aug;30(8):884–90.

181. Taylor WC, Smith RD. Solubility Characteristics of Glasses Basically Different in Composition*. Journal of the American Ceramic Society. 1936;19(1–12):331–5.

182. van Dijken JWV, Höglund-Åberg C, Olofsson A-L. Fired ceramic inlays: a 6-year follow up. Journal of Dentistry. 1998 Mar 1;26(3):219–25.

183. Morena R, Lockwood PE, Fairhurst CW. Fracture toughness of commercial dental porcelains. Dental Materials. 1986 Apr 1;2(2):58–62.

184. Rosenstiel SF, Gupta PK, Van Der Sluys RA, Zimmerman MH. Strength of a dental glass-ceramic after surface coating. Dental Materials. 1993 Jul 1;9(4):274–9.

185. Gehrt M, Wolfart S, Rafai N, Reich S, Edelhoff D. Clinical results of lithium-disilicate crowns after up to 9 years of service. Clin Oral Investig. 2013 Jan;17(1):275–84.

186. Chevalier J, Olagnon C, Fantozzi G. Subcritical Crack Propagation in 3Y-TZP Ceramics: Static and Cyclic Fatigue. Journal of the American Ceramic Society. 1999;82(11):3129–38.

187. Zhang Y, Lawn BR, Malament KA, Thompson VP, Rekow ED. Damage Accumulation and Fatigue Life of Particle-Abraded Ceramics. 2005;19(5):7.

188. Scherrer SS, Cattani-Lorente M, Vittecoq E, de Mestral F, Griggs JA, Wiskott HWA. Fatigue behavior in water of Y-TZP zirconia ceramics after abrasion with 30 μm silica-coated alumina particles. Dent Mater. 2011 Feb;27(2):e28-42.

189. Kosmač T, Oblak C, Jevnikar P, Funduk N, Marion L. The effect of surface grinding and sandblasting on flexural strength and reliability of Y-TZP zirconia ceramic. Dental Materials. 1999 Nov 1;15(6):426–33.

190. Scherrer SS, Cattani-Lorente M, Vittecoq E, de Mestral F, Griggs JA, Wiskott HWA. Fatigue behavior in water of Y-TZP zirconia ceramics after abrasion with 30 μm silica-coated alumina particles. Dent Mater. 2011 Feb;27(2):e28-42.

191. Kim M-J, Kim YK, Kim K-H, Kwon T-Y. Shear bond strengths of various luting cements to zirconia ceramic: Surface chemical aspects. Journal of Dentistry. 2011 Nov;39(11):795–803.

192. Braz R, Sinhoreti MAC, Spazzin AO, Loretto SC, Lyra AMV de C, Meira-Júnior D, et al. Shear bond strength test using different loading conditions - a finite element analysis. 2011 Jun 3 [cited 2017 Jun 30]; Available from: https://tspace.library.utoronto.ca/handle/1807/58379

193. The Arch, an Ultradent Blog - ISO Adopts Ultradent's Notched Edge Testing Method as Standard [Internet]. [cited 2019 Oct 16]. Available from: https://intl.ultradent.com/blog/Lists/Posts/Post.aspx?ID=115

194. Sorensen JA, Dixit NV. In vitro shear bond strength of dentin adhesives. Int J Prosthodont. 1991 Apr;4(2):117–25.

195. Pisaneschi E, Carvalho RCR de, Matson E. Shear bond strength of glass-ionomer cements to dentin: Effects of dentin depth and type of material activation. Revista de Odontologia da Universidade de São Paulo [Internet]. 1997 [cited 2020 Mar 20];11. Available from: http://www.scielo.br/scielo.php?script=sci_abstract&pid=S0103-06631997000500002&lng=en&nrm=iso&tlng=en

196. Meerbeek BV, Peumans M, Poitevin A, Mine A, Ende AV, Neves A, et al. Relationship between bond-strength tests and clinical outcomes. Dental Materials. 2010 Feb 1;26(2):e100–21.

197. Abi-Rached FO, Martins SB, Campos JA, Fonseca RG. Evaluation of roughness, wettability, and morphology of an yttria-stabilized tetragonal zirconia polycrystal ceramic after different airborne-particle abrasion protocols. J Prosthet Dent. 2014 Dec;112(6):1385–91.

198. Hallmann L, Ulmer P, Reusser E, Hämmerle CHF. Surface characterization of dental Y-TZP ceramic after air abrasion treatment. J Dent. 2012 Sep;40(9):723–35.

199. Ruyter EI, Vajeeston N, Knarvang T, Kvam K. A novel etching technique for surface treatment of zirconia ceramics to improve adhesion of resin-based luting cements. Acta Biomater Odontol Scand. 2017 Apr 14;3(1):36–46.

200. Huh Y-H, Park C-J, Cho L-R. Evaluation of various polishing systems and the phase transformation of monolithic zirconia. J Prosthet Dent. 2016 Sep;116(3):440–9.

201. Al-Haj Husain N, Camilleri J, Özcan M. Effect of polishing instruments and polishing regimens on surface topography and phase transformation of monolithic zirconia: An evaluation with XPS and XRD analysis. Journal of the Mechanical Behavior of Biomedical Materials. 2016 Dec;64:104–12.

202. Mohammadi-Bassir M, Babasafari M, Rezvani MB, Jamshidian M. Effect of coarse grinding, overglazing, and 2 polishing systems on the flexural strength, surface roughness, and phase transformation of yttrium-stabilized tetragonal zirconia. The Journal of Prosthetic Dentistry [Internet]. 2017 Apr [cited 2018 Apr 16]; Available from: http://linkinghub.elsevier.com/retrieve/pii/S0022391317300501

203. X-Ray Attenuation Length [Internet]. [cited 2020 Mar 21]. Available from: http://henke.lbl.gov/optical_constants/atten2.html

204. X-ray energy - GISAXS [Internet]. [cited 2020 Mar 21]. Available from: http://gisaxs.com/index.php/X-ray_energy

205. Hedegård B. Need for correlation between laboratory testing and clinical research. In: National Bureau of Standards Spec.

206. Inoue S, Koshiro K, Yoshida Y, Munck JD, Nagakane K, Suzuki K, et al. Hydrolytic Stability of Self-etch Adhesives Bonded to Dentin. J Dent Res. 2005 Dec 1;84(12):1160–4.

207. Munck JD, Landuyt KV, Coutinho E, Poitevin A, Peumans M, Lambrechts P, et al. Micro-tensile bond strength of adhesives bonded to class-I cavity-bottom dentin after thermo-cycling. Dental Materials. 2005 Nov 1;21(11):999–1007.

208. Eliasson ST, Dahl JE. Effect of thermal cycling on temperature changes and bond strength in different test specimens. Biomaterial Investigations in Dentistry. 2020 Jan 1;7(1):16–24.

209. Chen Y, Lu Z, Qian M, Zhang H, Chen C, Xie H, et al. Chemical affinity of 10-methacryloyloxydecyl dihydrogen phosphate to dental zirconia: Effects of molecular structure and solvents. Dental Materials. 2017 Dec 1;33(12):e415–27.

210. XPS Interpretation of Oxygen [Internet]. [cited 2019 Nov 11]. Available from: https://xpssimplified.com/elements/oxygen.php

211. Allen LC, Capitani JF, Kolks GA, Sproul GD. Van Arkel—Ketelaar triangles. Journal of Molecular Structure. 1993 Dec 3;300:647–55.

APPENDIX